

Aus der Klinik für Strahlentherapie und Radioonkologie
Direktor: Prof. Dr. Ch. Rube
Universitätsklinikum des Saarlandes, Homburg/Saar

**Analysis of DNA double-strand break repair
in spermatogonial stem cells within their physiological niche**

Dissertation zur Erlangung des Grades eines Doktors der Medizin
der Medizinischen Fakultät
der UNIVERSITÄT DES SAARLANDS

2010

Vorgelegt von: Sheng Zhang
geb. am 03.04.1975 in Wuhan, China

Index

1. ABSTRACT	- 1 -
1.1 Purpose	- 1 -
1.2 Materials and Methods	- 1 -
1.3 Results	- 1 -
1.4 Conclusion	- 2 -
2. INTRODUCTION	- 3 -
2.1. DNA double-strand breaks	- 3 -
2.1.1 An overview of DNA double-strand breaks	- 3 -
2.1.2 DNA double-strand breaks repair pathways	- 4 -
2.1.3 Proteins involved in the DSB repair	- 8 -
2.1.3.1 γ -H2AX	- 8 -
2.1.3.2 Mediator of Damage Checkpoint 1 (MDC1)	- 10 -
2.1.3.3 Tumor suppressor p53 binding protein1 (53BP1)	- 12 -
2.2 Germ cells and microenvironmental niche	- 14 -
2.2.1 Structure of the mouse testis	- 14 -
2.2.2 Spermatogenesis in mouse	- 16 -
2.2.3 Microenvironmental niche and SSCs self-renewal	- 20 -
2.3 DSB repair in male germ cells	- 23 -
2.4 Aim of the project	- 25 -
3. METHODS	- 26 -
3.1 Animals	- 26 -
3.2 Irradiation	- 26 -
3.3 Tissue sampling	- 27 -
3.4 Immunofluorescence staining in lung and kidney	- 27 -

3.5 Immunofluorescence double staining in testis	- 28 -
3.6 Determination of radiation-induced foci	- 28 -
3.7 Statistical analysis	- 29 -
4. RESULTS	- 30 -
4.1. Induction and repair of DSBs in normal tissues	- 30 -
4.2. Identification of undifferentiated spermatogonia by PLZF	- 33 -
4.3. Immunofluorescence staining in testis	- 33 -
4.4. DSB induction in testis	- 36 -
4.5. DSB kinetics in germ cells	- 37 -
5. DISCUSSION	- 39 -
5.1 DSB induction in mouse testis	- 39 -
5.2 DSB repair in differentiated round spermatids	- 40 -
5.3 DSB repair in undifferentiated spermatogonia	- 43 -
6. REFERENCES	- 46 -

Abbreviation

53BP1	tumor suppressor p53 binding protein 1
γ -H2AX	phosphorylated histone H2A.X
ATM	Ataxia-telangiectasia mutated
ATR	Ataxia-telangiectasia mutated Rad3-related
BRCA1	breast cancer susceptibility gene 1 protein
BRCT	BRCA1 C-terminal
CHK	checkpoint kinase
DDR	DNA-damage response
DNA-PK	DNA-dependent protein kinase
DNA-PKcs	catalytic subunit of DNA-dependent protein kinase
DSB	DNA double-strand break
GDNF	glial cell line-derived neurotrophic factor HR
LigIV	Ligase IV
MDC1	mediator of DNA damage checkpoint 1
MRN	MRE11-RAD50-NBS1 complex
NHEJ	non-homologous end-joining
PIKKs	phosphatidylinositol 3-kinase-related protein kinases
PLZF	promyelocytic leukemia zinc-finger
SCF	stem cell factor
SCID	severe combined immunodeficiency
SSB	DNA single-strand break
SSC	spermatogonial stem cell
WRN	Werner syndrome protein
XRCC4	X-Ray Repair Cross Complementing protein-4

1. Abstract

1.1 Purpose

Spermatogonial stem cells (SSCs) are the foundation of spermatogenesis. They and their direct descendants (A_{paired} and A_{aligned} spermatogonia), termed undifferentiated spermatogonia, reside in the basal compartment of seminiferous epithelium, known as stem cell niche. In the niche, SSC self-renewal and differentiation are regulated by intrinsic gene expression and extrinsic factors. The transcriptional repressor PLZF (promyelocytic leukemia zinc finger) is an essential regulator exclusively expressed in undifferentiated spermatogonia. By using PLZF immunofluorescence staining, we were able to distinguish undifferentiated spermatogonia from other spermatogonia, and analyzed DNA double-strand break (DSB) repair in spermatogonial stem cells within their physiological niche.

1.2 Materials and Methods

After whole body irradiation of repair-proficient mice, the induction and rejoining of DSBs were analyzed in PLZF-positive spermatogonia, compared to round spermatids and differentiated somatic cells by enumerating 53BP1 and γ -H2AX foci.

1.3 Results

DSB repair in male germ cells differs from that described for differentiated somatic cells. Different germ cell types express different DSB repair proteins, and no germ cell type possesses the complete set. Moreover, DSB repair in male germ cells was less efficient than in differentiated somatic cells. However, in PLZF-positive

SSCs, the DSB repair efficiency is clearly higher compared to other spermatogenic cells.

1.4 Conclusion

The compromised DSB repair efficiencies in male germ cells may result from the absence of some DSB repair proteins at the various developmental phases. Compared with round spermatids, DSB repair in PLZF-positive SSCs, however, is undoubtedly efficient, implying the important function of SSCs in maintaining the integrity of the genome.

2. Introduction

2.1. DNA double-strand breaks

2.1.1 An overview of DNA double-strand breaks

Of all types of DNA damage, DNA double-strand breaks (DSBs) are considered as the biologically most significant genotoxic lesions. If DSBs are not repaired accurately, this may result in serious consequences for cells, such as dysregulation of cellular functions, genomic instability, senescence or cell death (Morgan *et al.*, 1998; Olive, 1998). To protect the genome against these threatening events, a complex signal transduction cascade, known as DNA-damage response (DDR), initiates processes such as cell-cycle arrest, DNA repair and apoptosis before DNA replication and cell division (Kastan and Bartek, 2004). A vast network of proteins is involved in DDR and can be classified as sensors, mediators, transducers and effectors (Bekker-Jensen *et al.*, 2006) (Fig. 1). Sensors are defined as activities that can detect DNA lesions. Although the nature of sensors and the mechanisms of DNA-damage detection still remain unclear, the earliest detectable DSB-induced events have been found to involve the MRN complex (Rupnik *et al.*, 2008) and the PIKKs (phosphatidylinositol 3-kinase-related protein kinases) (Ward and Chen, 2001; Stiff *et al.*, 2004). From these proteins, the DNA-damage signal is transmitted to transducers such as checkpoint kinase 1 (CHK1) and checkpoint kinase 2 (CHK2), which function in signal transduction cascades targeting downstream DDR components, as well as amplifying DDR signals (Zhou and Elledge, 2000). The signalling between sensors and transducers is thought to be facilitated by mediator proteins such as MDC1 (mediator of DNA damage checkpoint protein 1), 53BP1 (tumor suppressor p53 binding protein 1) and BRCA1 (breast cancer susceptibility

gene 1 protein), thereby enhancing DDR signalling (Li and Zou, 2005). The activated sensors and transducers then target effectors, which initiate a series of events such as cell cycle arrest, DNA repair and apoptosis.

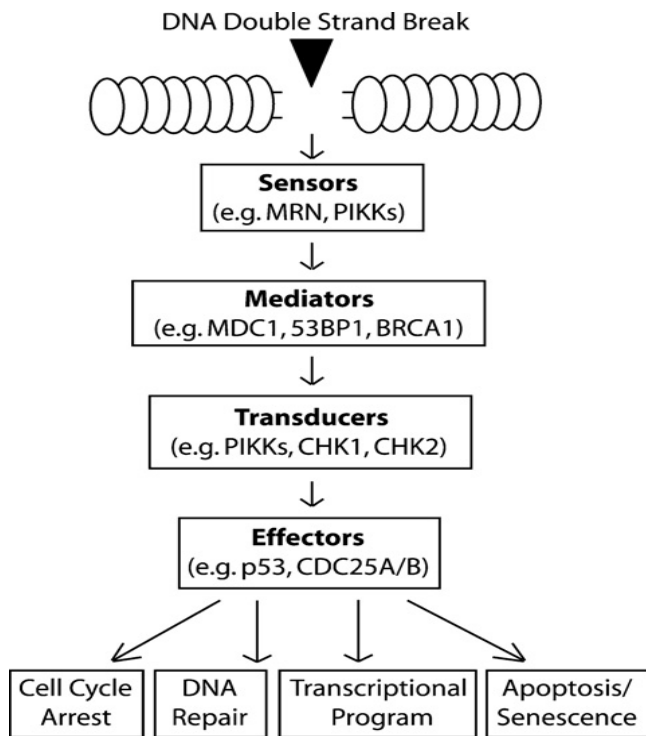


Figure 1: The DDR signal transduction cascade. Following DSB lesions, DNA damage is detected by sensor proteins, which transmit the damaging signal to a series of downstream effectors through a transduction cascade, to initiate processes such as cell-cycle arrest, DNA repair and apoptosis. Figure was taken from Fitzgerald *et al.*, 2009.

2.1.2 DNA double-strand breaks repair pathways

Upon exposure to DNA-damaging agents, eukaryotic cells repair DSBs primarily by two mechanisms: HR (homologous recombination) and NHEJ (non-homologous end-joining) (Jeggo, 1998; Johnson and Jasin, 2000). HR uses the sister chromatid or the homologous chromosome as a template for DSB repair. Therefore, the original DNA sequence can be precisely restored without the loss of information, based on homologous sequences (Johnson and Jasin, 2000). In contrast, NHEJ joins the broken ends without the need for homology, and thus is often associated with small deletions or insertions of nucleotides at the sites of repair. How cells make a choice between these two pathways to repair DSBs is quite complex and

not always clear (Shrivastav *et al.*, 2008). However, it has been shown that the relative contribution of HR and NHEJ to DSB repair depends on the cell type and the cell cycle phase. For instance, developing B and T cells preferentially use NHEJ to eliminate the DSBs in V(D)J recombination (Gellert, 2002; Lieber *et al.*, 2004), while spermatocytes undergoing meiotic divisions rejoin DSBs mainly by HR. In somatic cells, HR particularly occurs in dividing cells that are in S or G2 phase, in which undamaged sister chromatid can be employed as a template, whereas NHEJ can function throughout the whole cell cycle but predominately contributes to the DSB repair during G1 and G0 phases of the cell cycle, especially to most irradiation-induced DSBs (Aylon and Kupiec, 2005).

NHEJ in mammalian cells requires Ku (Ku70/80 heterodimer), DNA-PKcs (catalytic subunit of DNA-dependent protein kinase), XRCC4 (X-Ray Repair Cross Complementing protein-4), DNA LigIV (ligase IV) and Artemis (Lees-Miller and Meek, 2003; Weterings and van Gent, 2004; Mahaney *et al.*, 2009). As shown in Fig. 2, the first step in NHEJ is that DSBs are detected by Ku70/80 heterodimer, which has a high affinity for DNA ends and can form a ring around the DNA (Walker *et al.*, 2001). Ku70/80 binding on the site of the break facilitates the recruitment of DNA-PKcs. Together these three proteins constitute the DNA-PK (DNA protein kinase) complex. Activated DNA-PK complex recruits Artemis, XRCC4 and LigIV. Subsequently, XRCC4 and LigIV form a complex (XRCC4/LigIV complex), which catalyzes subsequent ligation of DNA ends to repair the breaks (Costantini *et al.*, 2007). It should be mentioned that a large fraction of DSBs needs to be processed by nucleases or polymerases before the XRCC4/LigIV complex joins the ends. Artemis is thought to be such a processing enzyme as remove nucleotides from the DNA ends by using its nuclease activity (Rooney *et al.*, 2003).

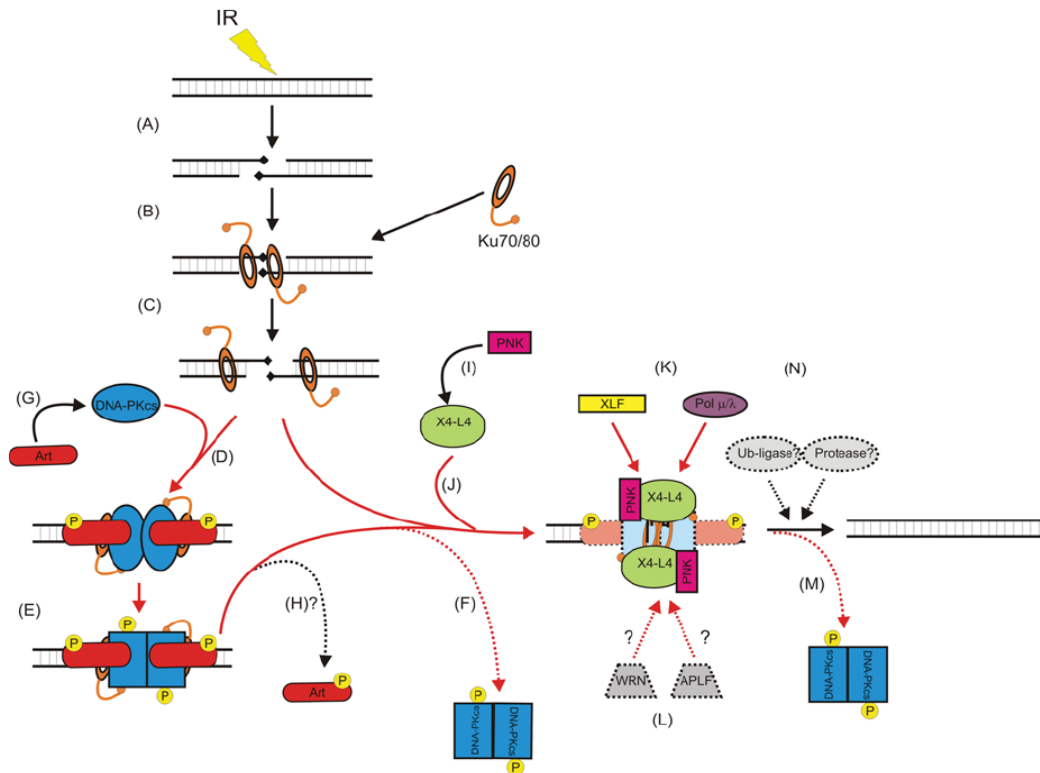


Figure 2: A model for NHEJ. (A) Irradiation induces multiple forms of DNA damage including DSBs. (B) The Ku heterodimer (orange) binds the ends of the DSB, tethering the ends together. (C) Ku translocates inwards, allowing the recruitment of DNA-PKcs (blue) such that it binds the extreme termini of the break. (D) Recruitment of DNA-PKcs to the DSB requires Ku, but no other NHEJ or DSB-repair factors. Two DNA-PK molecules (DNA-PKcs bound to DNA-bound Ku) interact to tether the DSB together. This triggers autophosphorylation (yellow circles) of DNA-PKcs. (E) A conformational change causes release of the DNA ends and/or release of phosphorylated DNA-PKcs from the complex. Whether DNA-PKcs is released prior to the recruitment of the XRCC4/LigIV complex (green) and its associated factors (F), or whether it remains part of a multi-protein complex until repair is completed (M) is not known. (G) A portion of the total cellular DNA-PKcs interacts with the nuclease Artemis (red), but if or when Artemis is released from the DNA-PKcs complex (H) is not known. (I) PNK (pink) interacts with XRCC4 suggesting that it is recruited to the break with the XRCC4/LigIV complex (green). (J) XLF (yellow) and DNA polymerase μ and λ (purple) interact with both XRCC4/LigIV and Ku, suggesting that they are recruited after or at the same time as XRCC4/LigIV is recruited to the Ku–DNA complex (K). Other processing enzymes such as WRN and APLF (grey) may also be recruited through interactions with DNA-bound Ku, XRCC4 and/or the XRCC4/LigIV complex (L). Once the ends are processed, the XRCC4/LigIV complex ligates the ends, repairing the break. Ligation of incompatible DNA ends is aided by the regulatory factor, XLF (K). How the various factors are released after repair is unknown. However, it is possible that ubiquitylation and/or proteolysis may be involved (N). Figure was taken from Mahaney *et al.*, 2009.

Mice deficient for Ku70 (Gu *et al.*, 1997), Ku80 (Nussenzweig *et al.*, 1996) or DNA-PKcs are viable but have defects in V(D)J recombination, and show marked

hypersensitivity to radiation. In addition, mice with defective DNA-PKcs, named SCID (severe combined immunodeficiency) mice, are fertile and exhibit a high rate of spontaneous apoptosis of spermatocytes in their testes (Gao *et al.*, 1998; Taccioli *et al.*, 1998; Hamer *et al.*, 2003).

In somatic cells, homologous recombination rejoins DSBs by using the sister chromatid as a template, and thus provides very high fidelity (West, 2003). As shown in Fig. 3, an early step in HR involves the generation of a single-stranded region of DNA, followed by the invasion of the template strand, which creates a Holliday junction. Subsequently, DNA synthesis by using a sister homolog is followed by branch migration and subsequent resolution of the heteroduplex. In the process of HR, RAD51 is a central player in promoting the strand invasion. BRCA2 is also required for HR and participates in the function of RAD51 (Pellegrini *et al.*, 2002). Other proteins involved in HR include RAD52, XRCC2, XRCC3, Mre11, Nbs1, etc. (San *et al.*, 2008).

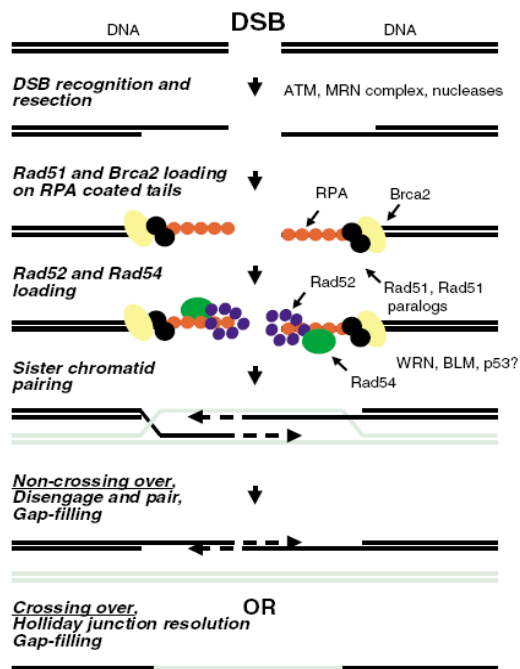


Figure 3: Homologous recombination. In the earliest stage, ATM senses and perhaps binds to the DSB, and phosphorylates H2AX, which would then attract BRCA1 and NBS1. The MRN complex resects the DNA to provide ssDNA overhangs necessary for DNA pairing and strand exchange. BRCA2, attracted to the DSB by BRCA1, facilitates the loading of RAD51 onto RPA-coated DNA overhangs with the help of RAD51 paralogs that in turn attract RAD52 and RAD54. The tumor suppressor p53, known to interact with BRCA1, RAD51, BLM and WRN, is also likely found in this DNA–protein complex. Figure was taken from Valerie *et al.*, 2003.

HR exerts a key function in rejoining DSBs that arise from replication-fork stalling (Alberts, 2003). Cells lacking HR are only mildly sensitive to ionizing radiation, but are highly sensitive to DNA-crosslinking agents (Thompson and Schild, 2001). This phenotype is consistent with the notion that the primary function of HR is to repair DSBs at replication forks while NHEJ primarily repairs DSBs generated elsewhere in DNA.

2.1.3 Proteins involved in the DSB repair

2.1.3.1 γ -H2AX

H2AX is a kind of histone H2A variant and constitutes 2–25% of mammalian histone H2A depending on the cell and tissue type (Rogakou *et al.*, 1998; Redon *et al.*, 2002). In response to DSBs, H2AX is rapidly phosphorylated at ser-129 in mouse (serine 139 in humans) by PIKK (phosphoinositide-3-kinase-related protein kinase) family members including ATM, ATR and DNA-PKcs (Rogakou *et al.*, 1998; Stiff *et al.*, 2004), leading to the formation of γ -H2AX foci at the sites of DSBs. In principle, all three PIKK members have the potential to phosphorylate H2AX. However, it has been reported that each of them actually carries out the phosphorylation when others are compromised (Andegeko *et al.*, 2001; Burma *et al.*, 2001; Stiff *et al.*, 2004; Wang *et al.*, 2005). ATM and DNA-PK display functional redundancy in phosphorylating H2AX after irradiation (Stiff *et al.*, 2004), while ATR appears more important for replication fork-associated damage and UV damage (Furuta *et al.*, 2003). H2AX phosphorylation is not limited to the immediate vicinity of the DSB site, but spreads from a few Mbp to many tens of Mbp in the chromatin regions surrounding the DSBs to form foci, which can be conveniently detected under immunofluorescence microscopy by using antibodies against γ -H2AX (Rogakou *et al.*, 1999; Pilch *et al.*, 2003). Discrete γ -H2AX foci appear immediately

following DSB generation, and reach maximal values within 10 to 30 minutes after radiation (Pilch *et al.*, 2003). The foci induced by radiation usually are referred to as irradiation-induced nuclear foci (IRIF) (Fernandez-Capetillo *et al.*, 2003; Fernandez-Capetillo *et al.*, 2004). It has been confirmed that the irradiation-induced γ -H2AX foci represent DSBs at a ratio of 1:1 even at low dose levels (Rothkamm *et al.*, 2003), and thus γ -H2AX has been utilized to quantify DSBs by counting the number of foci.

γ -H2AX plays an essential role in the recruitment and accumulation of DNA repair proteins to the sites of DSB damage (Paull *et al.*, 2000; Fernandez-Capetillo *et al.*, 2004; Fillingham *et al.*, 2006) and the sites of replication fork collapse (Furuta *et al.*, 2003). These DNA repair proteins colocalizing with γ -H2AX include 53BP1, MDC1, BRCA1, MRN complex, etc. By the combined use of relevant antibodies, it is possible to examine the co-localization of these DNA repair proteins by the immunofluorescence techniques (Sedelnikova *et al.*, 2003).

Once DSBs are repaired, γ -H2AX will be de-phosphorylated by protein phosphatases (PP2A and PP4) at 2 to 24 hours following irradiation (Bekker-Jensen *et al.*, 2006; Nakada *et al.*, 2008). It has been reported that the kinetics of γ -H2AX foci loss is related to the DSB repair capacity of both somatic cells (Nazarov *et al.*, 2003) and germ cells (Chicheportiche *et al.*, 2007). Persistent γ -H2AX foci following initial DSB induction indicate that some of the DSBs remain unrepaired, and thus are thought to be effective predictors of cellular response to radiation. After radiation, the delayed elimination of γ -H2AX foci is correlated with increased radiation sensitivity and decreased cell survival (Olive and Banáth, 2004; Liu *et al.*, 2008). Therefore, γ -H2AX has become an attractive candidate for the rapid assessment of radiation sensitivity in different types of cells (Marchetti *et al.*, 2006; Hamasaki *et al.*, 2007) and the identification of cells with defective DSB repair as well (Taneja *et al.*, 2004; Porcedda *et al.*, 2006; Porcedda *et al.*, 2009).

Lack of H2AX will diminish the recruitment of DNA repair proteins, leading to the impaired ability to DSB repair in cells. As shown in H2AX^{-/-} mice, they are radiosensitive, growth retarded, immune deficient, and male infertility (Bassing *et al.*, 2002; Celeste *et al.*, 2002).

2.1.3.2 Mediator of Damage Checkpoint 1 (MDC1)

At the sites of DSBs, MDC1 recognizes the γ -H2AX via its tandem BRCT (BRCA1 C-Terminal) domains, and then acts as a mediator protein, providing a 'landing-platform' for the binding of MRN (MRE11-RAD50-NBS1) complex (Stucki *et al.*, 2005; Lou *et al.*, 2006). Subsequent interactions between ATM and MDC1 lead to the further recruitment of activated ATM molecules to the vicinity of DSBs (DNA-PKcs and its interaction partner Ku might also be recruited by analogous mechanisms) (Lou *et al.*, 2004; Lou *et al.*, 2006). This further recruitment of PIKKs in turn phosphorylates additional H2AX molecules which are located more distal to the initiating lesions, and a positive feedback loop thus emerges (Stucki and Jackson, 2006) as shown in Fig. 4. Besides, increasing evidence indicates that MDC1 can directly interact with other proteins such as BRCA1, CHK2 and 53BP1 (Lou *et al.*, 2003; Xu and Stern, 2003). Similar to γ -H2AX, these proteins are also able to amplify the DNA damage signal for the recruitment of HR and/or NHEJ repair proteins. As a result, MDC1 plays an essential role in signal amplification even before the decision is made to repair via NHEJ or HR. By immunofluorescence staining, MDC1 foci can be detected in somatic cells after irradiation, overlapping with γ -H2AX and 53BP1 foci completely (Bhagal *et al.*, 2009). Loss of MDC1 expression or the reduction in levels of MDC1 by short-interfering RNA treatments leads to the decreased H2AX phosphorylation in response to irradiation. MDC1^{-/-} mice recapitulate many phenotypes of H2AX^{-/-} mice such as growth retardation,

male infertility, chromosome instability, immune defects, and increased radiosensitivity (Stewart *et al.*, 2003; Lou *et al.*, 2006).

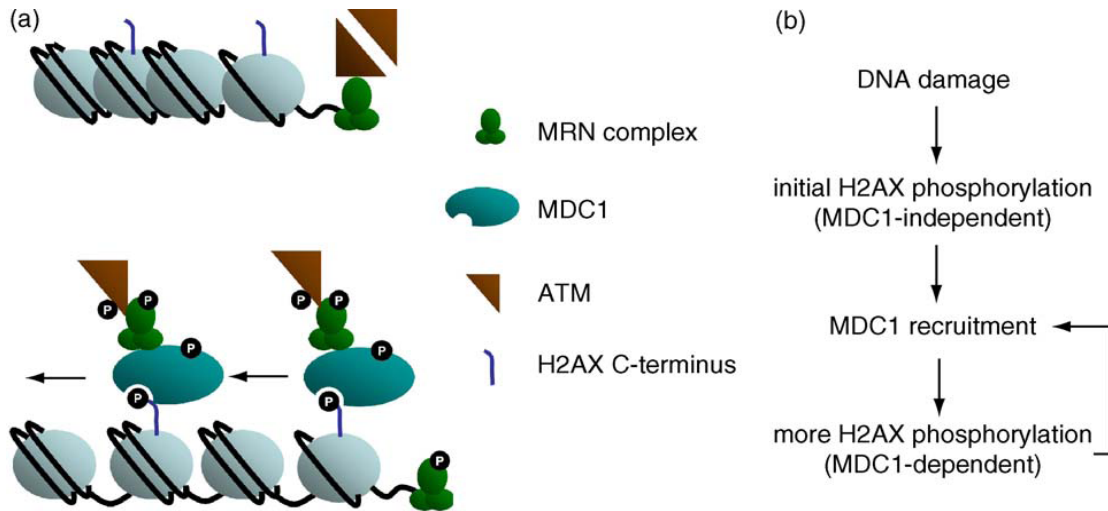


Figure 4: (a) Working model for regulation of H2AX phosphorylation by MDC1. Upper panel: initial recruitment of the MRN complex and ATM to free DNA ends. Lower panel: subsequent binding of MDC1, MRN complex and activated ATM to phosphorylated proximal H2AX, protection of the phosphorylated H2AX from access by PP2A and ‘spreading’ of H2AX phosphorylation in more distal chromatin regions. (b) Flow diagram of putative MDC1-dependent positive feedback loop that carries DNA damage-induced H2AX phosphorylation over large chromatin regions.

Figure was taken from Stucki and Jackson., 2006.

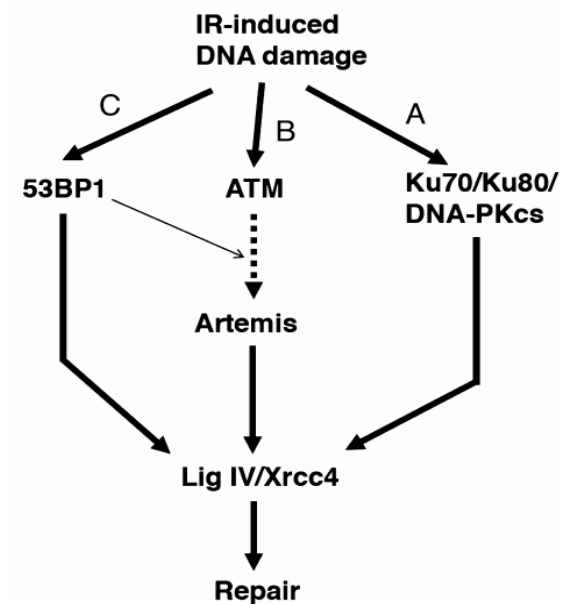


Figure 5: Model of DSB repair pathways for irradiation-induced DNA damage in G1 phase cells. A, B, C represent respectively the core NHEJ, ATM-Artemis-dependent and 53BP1-dependent pathways. The dotted arrow presents the minor pathway in DT40 cells. The thin arrow presents a possible interaction resulting from the scaffold function of 53BP1. Figure was taken from Kobayashi *et al.*, 2008.

2.1.3.3 Tumor suppressor p53 binding protein1 (53BP1)

After exposure to ionizing radiation, the tumor suppressor p53 binding protein 1 (53BP1) rapidly localizes to discrete foci at the sites of DSBs (Schultz *et al.*, 2000; Anderson *et al.*, 2001; Rappold *et al.*, 2001). The number of 53BP1 foci increases linearly with time, reaching a maximum within 15 to 30 minutes, and then steadily decreases to baseline levels within the next 16 hours (Schultz *et al.*, 2000). The maximum yield of 53BP1 foci, around 20 foci/cell/Gy, closely parallels the number of DSBs. Moreover, 53BP1 foci were observed to colocalize with γ -H2AX foci and MDC1 foci (Rogakou *et al.*, 1998; Bhogal *et al.*, 2009), suggesting that 53BP1 foci represent “sites of DSBs” and play an important role in the early response to DSBs.

The efficient recruitment of 53BP1 into focal structures after irradiation is a highly complex process involving multiple regulatory steps and interactions of various upstream factors such as γ -H2AX (Celeste *et al.*, 2003), MDC1 (Stewart *et al.*, 2003; Bekker-Jensen *et al.*, 2005). Lack of interactions with these factors will

impair the formation of 53BP1 foci. Celeste *et al.* reported that the initial recruitment of 53BP1 at the sites of DSBs is normal in H2AX $-/-$ mouse. However, 53BP1 fails to retain there, suggesting an essential role of γ -H2AX in the sustained retention of 53BP1 near the sites of DNA damage (Celeste *et al.*, 2003). In addition, the formation of 53BP1 foci is also impaired when cells are treated with wortmannin, an inhibitor of ATM, ATR and DNA-PK. As all these three kinases have the ability to phosphorylate H2AX, this effect of wortmannin is supposed to be by inhibition of H2AX phosphorylation (Schultz *et al.*, 2000; Ward *et al.*, 2003a).

Additionally, a direct interaction between the BRCT domains of MDC1 and amino acids residues 1288-1409 of 53BP1 may be required for the efficient formation of 53BP1 foci (Eliezer *et al.*, 2009). Stewart *et al.* reported that 53BP1 cannot localize to the sites of DSBs when MDC1 expression is suppressed by siRNA (Stewart *et al.*, 2003), in spite of contradictory observations made by other groups (Mochan *et al.*, 2004).

It is widely accepted that 53BP1 acts as a central mediator in the activation of DNA damage checkpoints, which lead to the arrest of cell cycle and make for the process of DSB repair. Moreover, increasing evidence suggests that 53BP1 also has the potential to participate in DSB repair directly (Fig. 5). Iwabuchi *et al.* found that the 53BP1 Tudor domains can stimulate the ligase activity of the DNA ligase IV/XRCC4 complex *in vitro* (Iwabuchi *et al.*, 2003; Iwabuchi *et al.*, 2006), suggesting the existence of a 53BP1-dependent pathway distinct from the core NHEJ pathway. In addition, 53BP1 was reported to contribute to NHEJ repair via an ATM-Artemis-Lig IV/XRCC4-dependent pathway, which is thought to reflect the late repair kinetics in G1 phase cells and may be involved in the DSB repair in heterochromatin (Goodarzi *et al.*, 2008; Kobayashi *et al.*, 2008).

Knockout or knockdown of 53BP1 will result in genome instability, as characterized by increased levels of chromatid gaps, breaks and exchanges, as well

as aneuploidy and tetraploidy even in the absence of exogenous DNA damage. Also, 53BP1-deficient mice and cell lines exhibit increased radiosensitivity to exogenous DNA damage (Ward *et al.*, 2003b; Nakamura *et al.*, 2006).

2.2 Germ cells and microenvironmental niche

2.2.1 Structure of the mouse testis

As shown in Fig. 6, mouse testis comprises two major parts: the seminiferous tubules and the interstitial tissue. The interstitial tissue is located in the area between seminiferous tubules, containing blood and lymphatic vessels that never penetrate the basal lamina of testis tubules. The seminiferous tubules are responsible for spermatogenesis. One mouse testis contains about 20 tubules, which are highly convoluted and are tightly packed inside the testicular capsule. Both ends of each tubule construct a loop structure connecting to the common outlet of mature sperm. In histology, the seminiferous tubule consists of seminiferous epithelium, basement membrane and myoid cells. The myoid cells connect each other to constitute a single cell layer surrounding the outside of basement membrane. As smooth muscle-like cells, myoid cells possess the ability to cause the contractions of seminiferous tubules, contributing to the movement of mature sperm to rete testis.

As the only somatic cell type within the seminiferous epithelium, Sertoli cell has an elongated cytoplasm extending from the basal lamina to the tubular lumen. The tight junctions between neighboring Sertoli cells constitute the anatomical basis of blood-testis barrier and next separate each seminiferous tubule into basal compartment and adluminal compartment (Dym and fawcett, 1970). The basal compartment (between the junctions and basement membrane) is occupied with spermatogonia containing SSCs (spermatogonial stem cells) and their differentiating progeny. In the early prophase of meiosis, preleptotene spermatocytes cross the tight

junctions and translocate to the adluminal compartment. In the adluminal compartment, spermatocytes undergo further development and give rise to round and elongating spermatids, which are continuously pushed up toward the tubular lumen during spermiogenesis. At the end of spermiogenesis, matured spermatozoa are released into the lumen, and then are transported to the epididymis. Obviously, the development of germ cells is closely associated with their surrounding structures constituted by Sertoli cells, which provide a physical and metabolic support during spermatogenesis.

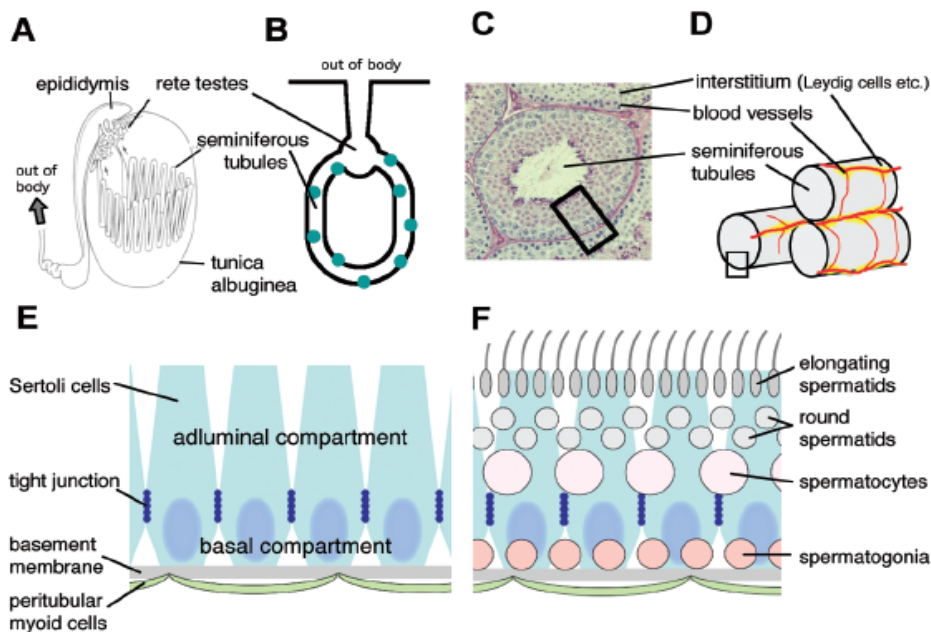


Figure 6: Anatomy of the mouse testis and seminiferous tubules. (A) Seminiferous tubules are highly convoluted and tightly packed in the tunica albuginea. (B) As shown by green dots, stem cells are scattered throughout the tubule loops. (C, D) The blood vessels (red) never penetrate the seminiferous tubule, but run through the interstitial space and form a network among the seminiferous tubules. (E) Anatomical framework composed of somatic components; (F) Spermatogenic cells in seminiferous epithelium. Figure was taken from Yoshida, 2008.

2.2.2 Spermatogenesis in mouse

Spermatogenesis is the process by which male spermatogonia develop into mature spermatozoa (Fig. 7). This process initiates in mouse embryo. After colonizing the genital ridge, primordial germ cells actively proliferate. Some of them undergo apoptosis, and the remainders convert to gonocytes. The gonocytes proliferate and subsequently arrest in G₀/G₁ phase. Shortly after birth, reactivated gonocytes migrate to the basal lamina of seminiferous tubules and afterwards differentiate into self-renewing spermatogonial stem cells (SSCs) by day 5 post-partum. Soon after the formation of SSCs, the first round of spermatogenesis occurs. Some of the SSCs differentiate and yield meiotic spermatocytes by day 10 post-partum. Meiotic phase lasts 10–12 days, leading to the appearance of haploid spermatids by day 21 post-partum. The spermatids further differentiate into mature spermatozoa, which first appear in seminiferous tubules by approximately day 35 post-partum. After this first round, SSCs enter spermatogenesis in a coordinated manner, which is related to a set of sophisticated control mechanisms in germ cells and leads to the continuous production of functional spermatozoa during the whole reproductive phase.

The entire process of mouse spermatogenesis takes about 35 days as described above, and can be divided into three sequential phases: 1, the mitotic proliferation phase; 2, the meiotic phase; 3, the post-meiotic phase of spermatid differentiation, named spermiogenesis.

The mitotic proliferation of spermatogonia starts with SSCs. They are single and isolated cells in morphology, and thus are called A_{single} spermatogonia (Oakberg, 1971; de Rooij, 1973). According to the most widely accepted model, the A_{single} spermatogonia can divide into two daughter cells. One of them remains as a stem cell, and the other enters the process of spermatogenesis and divides into paired A_{paired} spermatogonia (two cells connected by intercellular cytoplasmic bridges). The A_{paired}

spermatogonia next divide to form four long chains of aligned A_{aligned} cells (chains of 4 cells connected by intercellular bridges). Subsequent divisions form chains of 8 or 16 cells (Oatley and Brinster, 2006). A_{single} , A_{paired} , and A_{aligned} spermatogonia, also together termed undifferentiated spermatogonia, exhibit minimal heterochromatin condensation in their nucleus, and thus can be identified by morphological analysis under the electron microscopy or high-resolution light microscopy (Chiarini-Garcia and Russel, 2001; Chiarini-Garcia and Russel, 2002). The A_{aligned} spermatogonia subsequently initiate a differentiation step to convert to $A1$ spermatogonia. The $A1$ spermatogonia afterwards undergo five successive mitoses, giving rise to $A2$, $A3$, $A4$, intermediate and B spermatogonia (Ehmcke *et al.*, 2006). Finally, the B spermatogonia divide into primary preleptotene spermatocytes. This is the last mitotic division during spermatogenesis.

Meiosis is a highly coordinated cell division process, involving one round of DNA replication and two nuclear divisions called meiosis I and meiosis II (Olsen *et al.*, 2005). Similar to mitosis, both meiosis I and II can be divided into four stages: prophase, metaphase, anaphase, and telophase. The DNA replication before meiosis leads to the twice diploid DNA content ($2n$, $4c$ DNA) in primary spermatocytes in the preleptotene stage. Following preleptotene, the meiotic I prophase consists of five successive stages: leptotene, zygotene, pachytene, diplotene and diakinesis. In the leptotene stage, individual chromosomes condense into long filamentous strands to form a pair of sister chromatids attaching to the nuclear envelope by attachment plaques. Subsequently, the synapsis between homologous chromosomes occurs in the zygotene stage. Once the synapsis is completed, spermatocytes enter the pachytene stage, in which nonsister chromatids of homologous chromosomes randomly exchange the segments of genetic information over the regions of homology, while the heterologous XY chromosome pair only exchange information over a small region. Afterwards, the homologous chromosomes start to separate in the diplotene

stage, and two separated haploid secondary spermatocytes (1n, 2c DNA) appear in the diakinesis stage. Immediately, the second meiotic II division initiates. Sister chromatids are separated, leading to the formation of four haploid round spermatids (1n, 1c DNA).

As the last phase of spermatogenesis, spermiogenesis starts in round spermatids to form mature spermatozoa. Spermiogenesis is a complex process involving spermatid elongation, DNA condensation, and development of specific cellular structures, *etc.*, whereas a dramatic change of the chromatin structure takes place, including the transition of nucleohistone to nucleoprotamine. During the course of continuous DNA condensing, most of the somatic histones in round spermatids are replaced by testis-specific histone variants, which are subsequently replaced by transition proteins (TP1 and TP2) (Brewer *et al.*, 2002; Carrell *et al.*, 2007). In the elongating spermatid stages, the transition proteins are replaced by protamines, which allow the dense packaging of chromatin in spermatozoa. This condensed chromatin structure contributes to the protection of the genetic integrity during spermatozoon transport through the male and female reproductive tracts.

Because spermatogenesis is a rhythmic and cyclic process, male germ cells at the various phases are arranged in defined cellular associations in cross-sectioned seminiferous tubules, *i.e.* spermatogenic stages. Within a cycle of spermatogenesis, the number of stages differs between species. In mice, 12 stages have been defined and only one stage can be seen in one tubule cross section. Therefore, staging into the various spermatogenic stages provides an adjuvant method to recognize the different types of germ cells in seminiferous tubules.

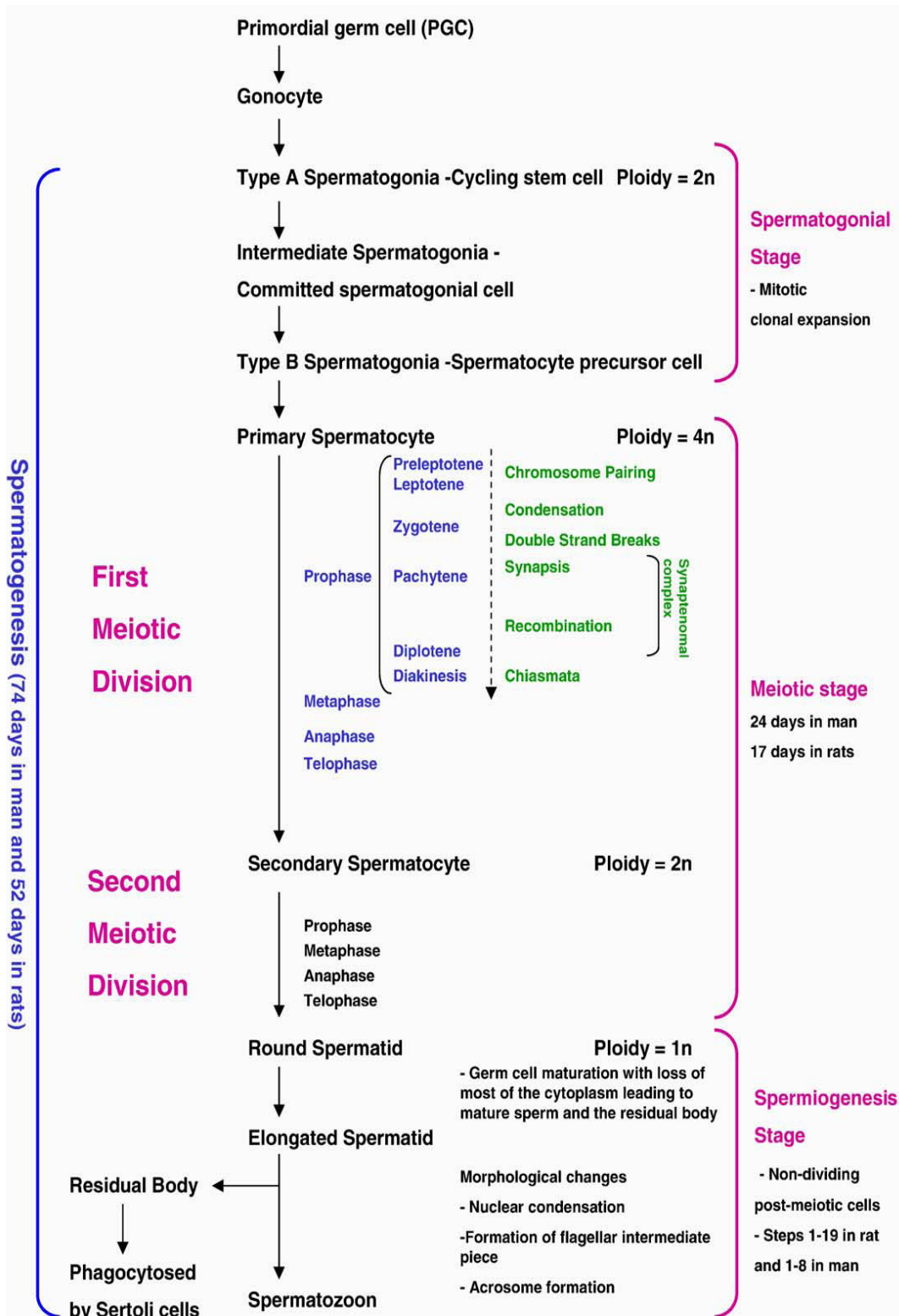


Figure 7: A schematic presentation of spermatogenesis. The general organization of spermatogenesis can be divided into three phases: the mitotic, the meiotic and the spermiogenesis stages. The mitotic proliferation stage starts with a division of spermatogonial stem cells into two daughter cells, one of which enters the process of spermatogenesis, while the other remains as a stem cell. This is the period of active replicative DNA synthesis producing different types of spermatogonia. The ultimately type B spermatogonia give rise to tetraploid primary spermatocytes in the preleptotene stage. During the first prophase of the meiotic stage, genetic recombination takes place after which a first reduction division gives rise to secondary $2n$ spermatocytes, and subsequently the second reduction division results in haploid round spermatids. During spermiogenesis, extensive changes occur in spermatids, including nuclear condensation, leading to spermatozoa. Figure was taken from Olsen *et al.*, 2005.

2.2.3 Microenvironmental niche and SSCs self-renewal

Stem cells are defined as a group of undifferentiated cells having the dual ability to renew themselves by mitotic division and to differentiate into functional mature cells. In adult tissues, stem cells reside in a physiologically limited microenvironment called stem cell niche, in which stem cells can be maintained throughout their lifespan. The specialized environment in the niche will promote stem cell self-renewal, whereas stem cells leaving the niche will most likely get into an environment promoting their differentiation. It has been reported that the activities of different kinds of stem cells are sophisticatedly regulated within their niches in several organs such as gonads, skin and intestine (Spradling *et al.*, 2001), even though these stem cell niches vary in nature and location depending on the tissue type (Li and Xie, 2005).

On the basis of experimental results obtained by post-transplantation spermatogenic colony formation (Brinster and Avarbock, 1994; Brinster and Zimmermann, 1994; Brinster, 2002), it has been widely accepted that A_{single} spermatogonia, a morphological subtype of undifferentiated spermatogonia, are the SSCs in mouse testis. Undifferentiated spermatogonia (A_{single} , A_{paired} , and A_{aligned} spermatogonia) can be morphologically distinguished from A1 to B spermatogonia

in testis sections by a special fixative and embedding technique (Chiarini-Garcia *et al.*, 2001; Chiarini-Garcia *et al.*, 2002). The distribution of undifferentiated spermatogonia is not random in mouse seminiferous tubule. The vast majority of them resides in the basal compartment, which are adjacent to the blood vessels and interstitial tissue and be regarded as the niche for undifferentiated spermatogonia (Yoshida *et al.*, 2007) (Fig. 8). Further analysis showed that the A_{single} spermatogonia are preferentially located along the basal membrane opposing blood vessels, while A_{aligned} spermatogonia are localized in the areas opposed to blood vessels (Shetty and Meistrich, 2007).

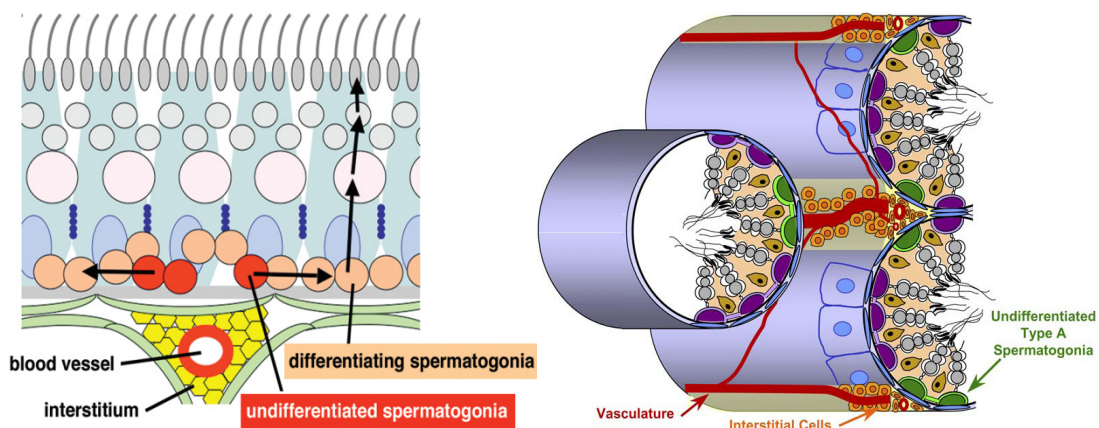


Figure 8: Schematic model of the niche microenvironment for undifferentiated spermatogonia.

The basal compartment adjacent to blood vessels and interstitial tissue is regarded as the niche for undifferentiated spermatogonia. Upon transition into A_1 , they migrate horizontally to spread throughout the basal compartment, followed by six mitotic divisions in the basal compartment and subsequent vertical translocation into the adluminal compartment upon entering meiosis.

Figure was taken from Yoshida *et al.*, 2008.

The SSCs are the foundation of spermatogenesis. They can self-renew and generate a large number of differentiated germ cells. A balance between SSCs self-renewal and differentiation in adult testis is essential for the maintenance of

normal spermatogenesis. This balance is strictly regulated by the intrinsic gene expression in SSCs and extrinsic signals including a number of soluble factors from the surrounding niche. It has been confirmed that most of the presently known factors are produced by Sertoli cells (de Rooij, 2009). Some of these factors (GDNF (glial cell line-derived neurotrophic factor) and FGF2 (fibroblast growth factor 2)) stimulate the self-renewal and proliferation of SSCs, others (SCF (stem cell factor), BMP4 (bone morphogenetic protein 4), and Activin A) induce the differentiation, suggesting that Sertoli cells are the major contributors to the niche regulation. Among these factors, the regulating effects of GDNF have been well understood (Meng *et al.*, 2000; Sariola and Saarma, 2003). Heterozygous GDNF knockout mice show a progressive depletion of SSCs (Meng *et al.*, 2000). Conversely, the mice overexpressing GDNF exhibit an increased number of undifferentiated spermatogonia, resulting in the seminoma (Meng *et al.*, 2001). It should be mentioned that the secretion of GDNF is under the control of FSH (follicle-stimulating hormone) blood levels (Tadokoro *et al.*, 2002). This might be one of the reasons why the SSC niche is close to the blood vessels and interstitial tissue.

The intrinsic gene expression in SSCs also plays an essential role in the regulation of SSC behavior. Mice with Luxoid mutant exhibit a progressive loss of SSCs after birth. PLZF (promyelocytic leukemia zinc finger protein), a kind of transcriptional repressor protein originally identified in haematopoietic cells (Reid *et al.*, 1995), has been confirmed to be the disrupted gene in the luxoid mutation (Buaas *et al.*, 2004; Costoya *et al.*, 2004). The PLZF is exclusively expressed in A_{single} , A_{paired} , and A_{aligned} spermatogonia (Payne and Braun, 2006). Filipponi *et al.* recently reported that PLZF can directly inhibit the transcription of c-Kit receptor in A_{single} , A_{paired} and A_{aligned} spermatogonia (Filipponi *et al.*, 2007). The c-Kit receptor is expressed from late A_{aligned} spermatogonia onwards, and plays an important role in the transition of A_{aligned} spermatogonia into A1 spermatogonia after activation by its

ligand: stem cell factor (SCF) (Schrans-Stassen *et al.*, 1999). In view of this, PLZF prevents A_{single} , A_{paired} and A_{aligned} spermatogonia to differentiate into A1 spermatogonia probably by inhibiting the transcription of c-Kit receptor in undifferentiated spermatogonia. Loss of PLZF function in undifferentiated spermatogonia will shift the strictly regulated balance between self-renewal and differentiation towards differentiation, finally resulting in the depletion of SSCs and male sterility.

In view of the fact that spermatogonia consist of various subtypes, the identification and purification is an important precondition for the study of SSCs *in vitro* and *in vivo*. The unequivocal expression of given surface markers in spermatogonia will help us to identify some subtypes of spermatogonia. Fluorescence-activated cell sorting with c-kit was used to enrich type A1-A4 spermatogonia from mouse testis; Yoshida *et al.* found that Ngn3 (neurogenin3), a basic helix-loop-helix transcription factor, is expressed in undifferentiated spermatogonia, and successfully visualized these spermatogonia by GFP (green fluorescent protein) labeling technique (Yoshida *et al.*, 2007). In the present study, by using the PLZF immunofluorescence staining of mouse testis sections, we were able to distinguish undifferentiated spermatogonia from other subtypes. This approach allowed us to analyze the DSB repair of undifferentiated spermatogonia *in vivo*.

2.3 DSB repair in male germ cells

DNA double-strand breaks can be caused by exogenous agents such as oxidative radicals and ionizing radiation, and can arise endogenously during DNA replication, V(D)J recombination, and meiotic recombination in male germ cells (Hoeijmakers, 2001; van Gent *et al.*, 2001). The accurate repair of these endogenous DSBs is critical for male germ cells to avoid reproductive failure and abnormal

chromosomal alternations. Meiosis-specific homologous recombination is a distinct DSB repair mechanism that occurs between homologous chromosomes during meiotic prophase I. Recent studies have shown that the SPO11 protein, a member of topoisomerase family, plays an important role in the generation of endogenous DSBs, which are thought to be the starting points of homologous recombination. Subsequent procedures require homologous chromosome as a template and the participation of proteins such as RAD51 and DMC1. The detailed repair process of meiotic recombination is similar but not totally identical to HR in somatic cells (Li and Ma, 2006).

Upon exposure to exogenous damages such as ionizing radiation, eukaryotic cells repair DSBs primarily by two pathways: HR and NHEJ (Jeggo, 1998; Johnson and Jasin, 2000). Although both pathways are important, it has been known that the relative contribution of HR or NHEJ to DSB repair depends on the cell type and the cell cycle phase. HR particularly occurs in S and G2 phase, while NHEJ is active throughout the cell cycle but predominately in G1 and G0 phase (Rothkamm and Löbrich, 2003). In regard to male germ cells, which comprise various types, apparently, the choice of DSB pathway must differ in different types. Both pathways seem to be possible in the contiguous differentiating spermatogonia undergoing mitotic divisions. However, in undifferentiated spermatogonia, it has been reported that most of them actually stay in a quiescent state, only less than 10% divides per day (Tegelenbosch and de Rooij, 1993). Therefore, NHEJ is believed to be a more important pathway for undifferentiated spermatogonia to rejoin DSBs relative to HR. As mentioned above, the meiotic homologous recombination is the predominant pathway in spermatocytes undergoing meiosis, especially from the leptotene to middle pachytene stages. In haploid spermatids, the homologous recombination seems to be impossible due to the absence of sister chromatids and homologous chromosomes.

Moreover, recent studies have shown that the expression of DSB repair proteins differs in the various types of male germ cells. This may also influence the choice of DSB repair pathways as well as the repair efficiency. For example, Ku70, an indispensable protein in NHEJ, is absent during early prophase I, leading to a shift towards HR by suppressing NHEJ pathway (Goedecke *et al.*, 1999; Hamer *et al.*, 2003). On account of the fact that the endogenous DSBs arise naturally in this period, it is helpful for spermatocytes to minimize the germline mutations by utilization of error-free HR mechanism. In contrast, Ku70 is expressed in round spermatids. However, immunohistochemical evidence has indicated that DNA-PKcs is absent in these haploid cells (Hamer *et al.*, 2003), suggesting an impaired repair efficiency of NHEJ. In addition, Ahmed *et al.* recently reported that the expression of MDC1 and 53BP1 differs for the various male germ cell types, leading to different DSB repair capacities (Ahmed *et al.*, 2007).

2.4 Aim of the project

Spermatogonial stem cells are the foundation of spermatogenesis, and thus have an important function in maintaining the integrity of genome. In mouse testes, SSC self-renewal and differentiation are sophisticatedly regulated in the stem cell niche by intrinsic gene expression and extrinsic signaling factors. PLZF is an essential regulator exclusively expressed in undifferentiated spermatogonia. By the established double staining for PLZF combined with γ -H2AX and 53BP1, this study aimed to analyze the DSB repair in SSCs within their physiological niche.

3. Methods

3.1 Animals

Male C57BL/6 (wild-type, C57BL/6NCrl) mice of different ages (2 weeks, 8 weeks and 12 weeks) were obtained from Charles River Laboratories (Sulzfeld, Germany). All mice were housed 4-5 per cage in laminar flow hoods under identically standard laboratory conditions (temperature $22 \pm 2^\circ\text{C}$, humidity $55 \pm 10\%$, and light-dark cycle 12:12), and had free access to sterilized food and water. Before use, the mice were allowed to acclimatize from shipping for 1 week. The experimental protocol was approved by the Animal Care and Use Committee of the Saarland University.

3.2 Irradiation

Whole body irradiation was performed in a special plastic cylinder with a 6-MV linear accelerator at a dose rate of 2 Gy/min. The isodose distributions were evaluated by ADAC Pinnacle three-dimensional treatment planning system, revealing that the 95% isodose enclosed the whole body of each individual mouse. Before irradiation, all mice were randomly placed into appropriate treatment groups. For the DSB induction, three 8-week-old mice per dose group (0.01 Gy, 0.1 Gy, 0.5 Gy and 1 Gy) were sacrificed at 30 min after irradiation. For the DSB repair kinetics, three 12-week-old mice per time point were sacrificed at 0.5 h, 5 h, 24 h and 48 h after irradiation with 1 Gy. In each case, three sham-irradiated mice served as controls.

3.3 Tissue sampling

After anesthesia (intraperitoneal injection of Rompun and Ketamine; Rompun 1ml and Ketamine 0.75 ml, diluted in 8.25 ml 0.9% sodium chloride solution; 0.1 ml/10 g body weight), the organs (testis, lung and kidney) were immediately removed and placed in fixative (4% neutral buffered formaldehyde) for 16 h at room temperature. After dehydration with a graded series of ethanol and xylene by an automatic tissue dehydration apparatus, the organs were embedded in paraffin and were sectioned at an average thickness of 4 μm .

3.4 Immunofluorescence staining in lung and kidney

To analyze the induction and repair of DSBs in the differentiated cells of lung and kidney, we performed the immunofluorescence staining with antibodies against 53BP1 and γ -H2AX according to the following protocol:

Paraffin sections were dewaxed twice in 100% xylene (10 min each), and hydrated by progressively washing with absolute ethanol, 96% ethanol, 90% ethanol, 80% ethanol, 70% ethanol and distilled water (5 min each), and then boiled in the citrate buffer (DAKO Retrieval puffer, #S-2031, Glostrup, Denmark) for 60 min at 96°C to unmask the antigenic sites. After 20 min cooldown at room temperature, sections were soaked in the normal goat serum (#642921 ICN, Irvine, CA, USA) at room temperature for 60 min to block non-specific binding sites. Afterwards, the sections were incubated with the primary rabbit polyclonal antibody against 53BP1 (Bethyl, #IHC-0001 Montgomery, TX.) at a 1:200 dilution in a humidified chamber overnight at 4°C, and were next incubated with Alexa Fluor 488-conjugated goat anti-rabbit secondary antibody (Invitrogen, cat #A11008) at a 1:400 dilution in a humidified chamber for 60 min in dark at room temperature. Finally, the sections were mounted in DAPI-containing mounting medium (Vector Laboratories,

Burlingame, CA) and were stored at 4°C until use. Between each step, the sections were gently washed with PBS three times (10 min each) on a shaker.

Similar steps were taken for immunofluorescence staining with antibody against γ -H2AX, except for the use of the primary rabbit polyclonal antibody against γ -H2AX (Bethyl, #IHC-0059, Montgomery, TX) at a 1:200 dilution.

3.5 Immunofluorescence double staining in testis

Considering the exclusive expression of PLZF in undifferentiated spermatogonia, we performed the immunofluorescence double stainings (PLZF/53BP1 and PLZF/ γ -H2AX) in the testis. Sections were incubated in the mixture of two primary antibodies (mouse monoclonal antibody against PLZF, Calbiochem, San Diego, CA, at a 1:50 dilution; rabbit polyclonal antibody against 53BP1 or γ -H2AX, both at a 1:200 dilution) overnight at 4°C, and were next incubated in the mixture of two secondary antibodies (Alexa Fluor-568-conjugated goat anti-mouse and Alexa Fluor-488 conjugated-conjugated goat anti-rabbit, both at a 1:400 dilution, Invitrogen) for 60 min at room temperature in dark.

3.6 Determination of radiation-induced foci

The sections were examined by using a Nikon E600 epifluorescent microscope equipped with charge-coupled device camera and acquisition software (Nikon, Düsseldorf, Germany). For quantitative analysis, 53BP1 and γ -H2AX foci were counted by eye under x600 microscope magnification. For each data point, the lung, kidney and testis sections from three different mice were analyzed. Foci/cell counting was performed until at least 50 cells and 40 foci were registered for each sample. The number of PLZF-positive cells per seminiferous tubule also was counted in the testis sections.

3.7 Statistical analysis

To evaluate the potential differences in DSB rejoining kinetics between spermatogonial stem cells, round spermatids and differentiated somatic cells. The Mann-Whitney U test was performed for each time-point (0.5 h, 5 h, 24 h and 48 h post-irradiation). The criterion for statistical significance was $p \leq 0.05$.

4. Results

4.1. Induction and repair of DSBs in normal tissues

To investigate the induction and repair of DSBs in differentiated somatic cells, we performed the 53BP1 immunofluorescence staining in the lung and kidney sections. The absolute number of 53BP1 foci per cell was counted by eye in renal tubular epithelial cells and bronchiolar epithelial cells, respectively.

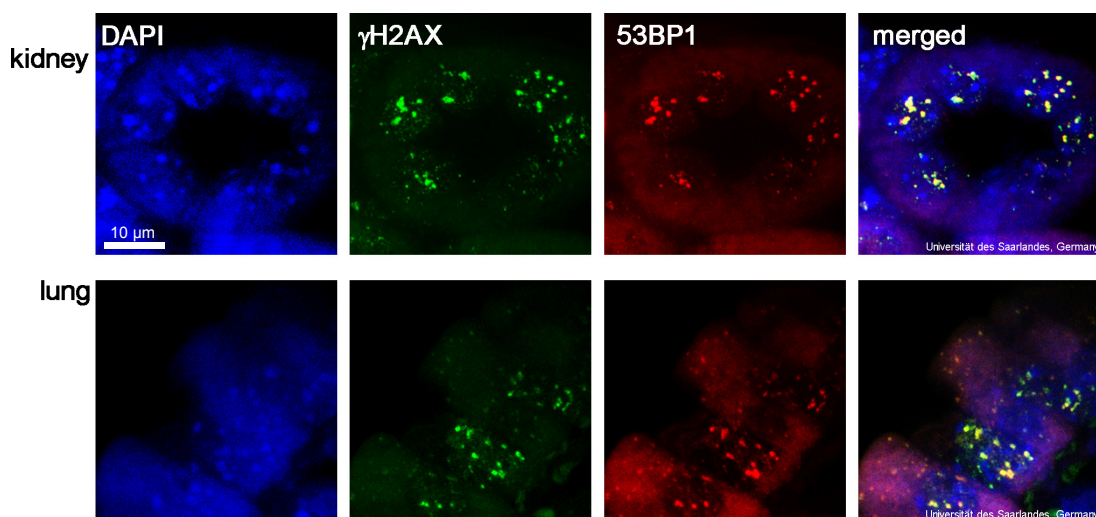


Figure 9: Immunofluorescence staining of γ -H2AX (green) and 53BP1 (red) in kidney and lung tissues at 0.5 h after whole body irradiation with 1 Gy. DNA counterstained with DAPI (blue), and images merged to determine co-localization (yellow). Clear 1:1 co-localization between γ -H2AX and 53BP1 manifested in both analyzed tissues.

As shown in Fig. 9, thirty minutes after exposure to irradiation, the numbers of 53BP1 foci clearly increased in both lung and kidney sections, while the unirradiated controls were predominantly negative for 53BP1. By enumerating foci, we observed very low background levels in controls (0.04 foci/cell) and a linear correlation between the foci formation and the radiation dose in both tissues, with approximately 1 foci/cell after 0.1 Gy, 4.5 foci/cell after 0.5 Gy, 7.5 foci/cell after 1 Gy (Fig. 10).

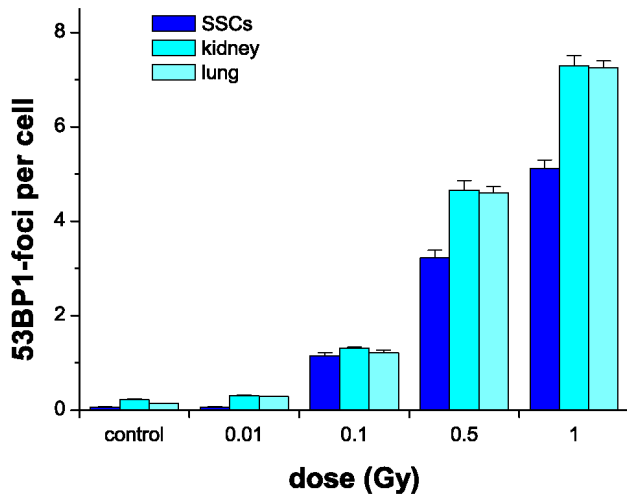


Figure 10: DSB induction quantified by enumerating **53BP1** foci in SSCs, as well as the differentiated somatic cells in kidney and lung at 30 min after whole body irradiation. All analyzed cell types revealed linear dose correlation from 0.1 Gy to 1.0 Gy. Error bars represent standard error of mean from three experiments.

These data are in line with the previous results obtained by γ -H2AX staining (Rübe *et al.*, 2008b), indicating that 53BP1 immunofluorescence analysis can be used to quantify the radiation-induced DSBs in both analyzed tissues.

We next counted the 53BP1 foci at defined time points (0.5 h, 5 h, 24 h and 48 h) after irradiation with 1 Gy. As shown in Fig. 11, both kinds of the tissues exhibited similar kinetics for 53BP1 foci elimination. The average number of foci per

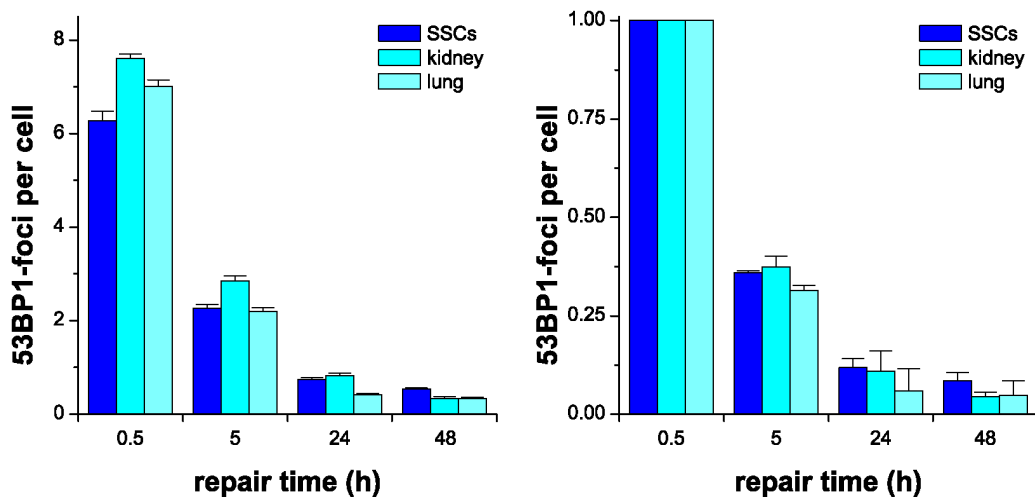


Figure 11: DSB repair kinetics of SSCs compared with differentiated somatic cells (lung and kidney) by counting **53BP1** foci at defined time-points (0.5 h, 5 h, 24 h and 48 h) after irradiation with 1 Gy. Moderate increased residual 53BP1 foci levels were observed in SSCs at 24 h and 48 h time points. Error bars represent standard error of mean from three experiments.

cell peaked at 30 min after irradiation (7.5 foci/cell), and approximately 30% of the peak-value was observed at 5 h post-irradiation (2.5 foci/cell). At 24 h and 48 h, only a few foci remained (0.5 foci/cell and 0.3 foci/cell), suggesting that most of the radiation-induced DSBs had been repaired before 24 h post-irradiation.

γ -H2AX, a widely accepted marker for DSBs, also was analyzed at each observation point along with the analysis of 53BP1. Fig. 9 shows the nearly 1:1 co-localization of γ -H2AX and 53BP1 foci in both tissues. Moreover, the elimination kinetics of γ -H2AX foci was in line with that of 53BP1 foci (Fig. 12). No significant variations in the initial yields of γ -H2AX or 53BP1 foci were observed in both analyzed tissues. These results strengthen the notion that the DSB rejoining kinetics in differentiated somatic cells are nearly identical (Rübe *et al.*, 2008b).

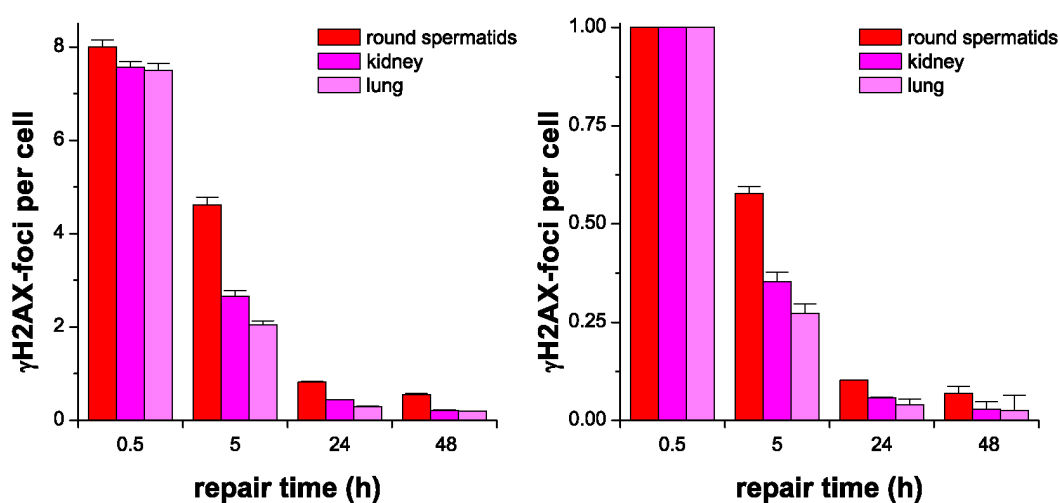


Figure 12: DSB repair kinetics of round spermatids compared with differentiated somatic cells (lung and kidney) by counting γ -H2AX foci at defined time-points (0.5 h, 5 h, 24 h and 48 h) after irradiation with 1 Gy. Increased γ -H2AX foci levels were observed in round spermatids at 5 h, 24 h and 48 h time points, suggesting that DSB repair in round spermatids is clearly less efficient than analyzed somatic cells. Error bars represent standard error of mean from three experiments.

4.2. Identification of undifferentiated spermatogonia by PLZF

It has been reported that PLZF plays an essential role in the maintenance of SSC self-renewal. The expression of PLZF is restricted to the subtypes of spermatogonia exhibiting stem cell-like properties (Payne and Braun, 2006). Using immunohistochemical staining by mouse anti-PLZF antibodies, we observed that PLZF is exclusively expressed in A_{single} , A_{paired} and A_{aligned} spermatogonia located near the basement membrane of seminiferous tubules.

By immunofluorescence staining, we calculated the average numbers of PLZF positive cells per tubule at different ages. In immature 2-week-old mice, around 4 PLZF-positive spermatogonia were detected per tubule. In contrast, the average number in 12-week-old mice was much lower, with approximately 0.5 cells per tubule. This age-dependent decline of PLZF-positive spermatogonia per tubule is in line with the features of pubertal development in mouse testis (de Rooij and Russell, 2000). Our results, therefore, suggest that PLZF immunofluorescence staining can be used as a feasible approach to distinguish undifferentiated spermatogonia from other types of germ cells in mouse testis sections. By the established immunofluorescence double stainings (PLZF/53BP1 and PLZF/ γ -H2AX), we were able to analyze the DSB repair of SSCs within their physiological niche.

4.3. Immunofluorescence staining in testis

As shown in Fig. 13. In the unirradiated testis sections, strong homogeneous nuclear staining and pronounced γ -H2AX foci were observed in the preleptotene and leptotene spermatocytes. From the zygotene to pachytene stages, the numbers of γ -H2AX foci decreased gradually, and an intensive γ -H2AX staining localized in sex chromosome, which can be easily recognized in morphology. In late pachytene spermatocytes, only the sex vesicles were stained, and this staining disappeared in

diplotene spermatocytes (stage XII of the cycle of the seminiferous epithelium). In some given spermatogenic stages, round spermatids regularly exhibited a weak homogeneous nuclear staining and some dispersed tiny foci. It should be noted that these tiny foci were significantly weaker and smaller than those irradiation-induced foci. Late elongated spermatids and all somatic cells (*i.e.* myoid, Leydig and Sertoli cells) were negative for γ -H2AX. After carefully examining the sections, we found that γ -H2AX-positive and negative spermatogonia both existed in testis sections, suggesting the existence of different γ -H2AX expression patterns in spermatogonia subtypes. By PLZF/ γ -H2AX double staining, we found that all of the PLZF-positive spermatogonia (*i.e.* undifferentiated spermatogonia) were definitely negative for γ -H2AX staining.

After irradiation with defined doses, all of the spermatocytes, round spermatids and PLZF-negative spermatogonia exhibited striking radiation-induced γ -H2AX foci in their nuclei, whereas no γ -H2AX foci was detected in PLZF-positive spermatogonia and elongated spermatids.

To better know the expression of DSB repair proteins in different germ cell types, we next performed the PLZF/53BP1 double staining in testis sections. In the controls, diffuse nuclear staining for 53BP1 was observed in both PLZF-positive and negative spermatogonia, pachytene and diplotene spermatocytes, and round spermatids. The sex vesicles showed an intense 53BP1 staining in late pachytene spermatocytes. After irradiation, 53BP1 foci rapidly appeared in all spermatogonia, preleptene spermatocytes and late pachytene spermatocytes, but failed to be detected in any other germ cell types. In addition, we noticed that the PLZF positive spermatogonia exhibited a kind of uniform pale nuclear staining with DAPI, and strong background staining of 53BP1. These were clearly different from that in PLZF-negative spermatogonia and differentiated somatic cells (Fig. 14).

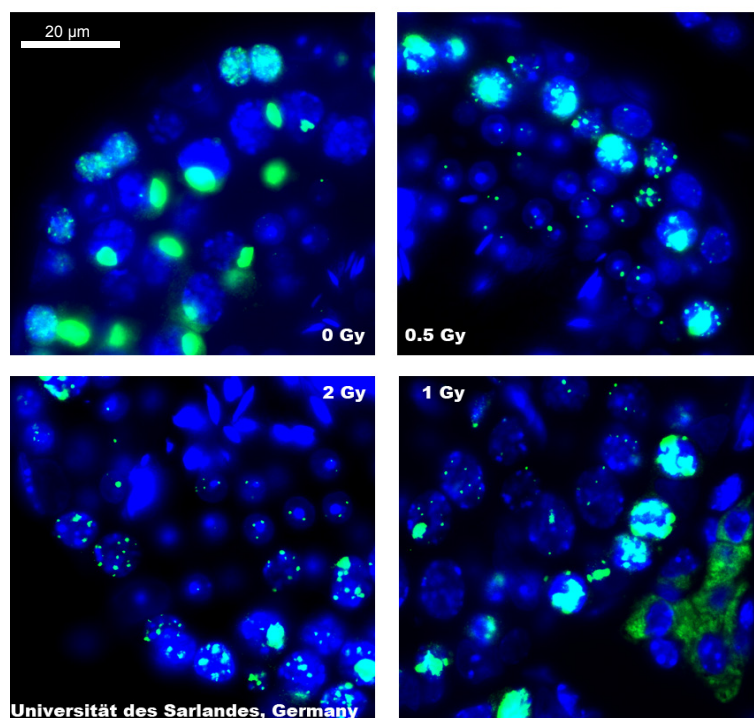
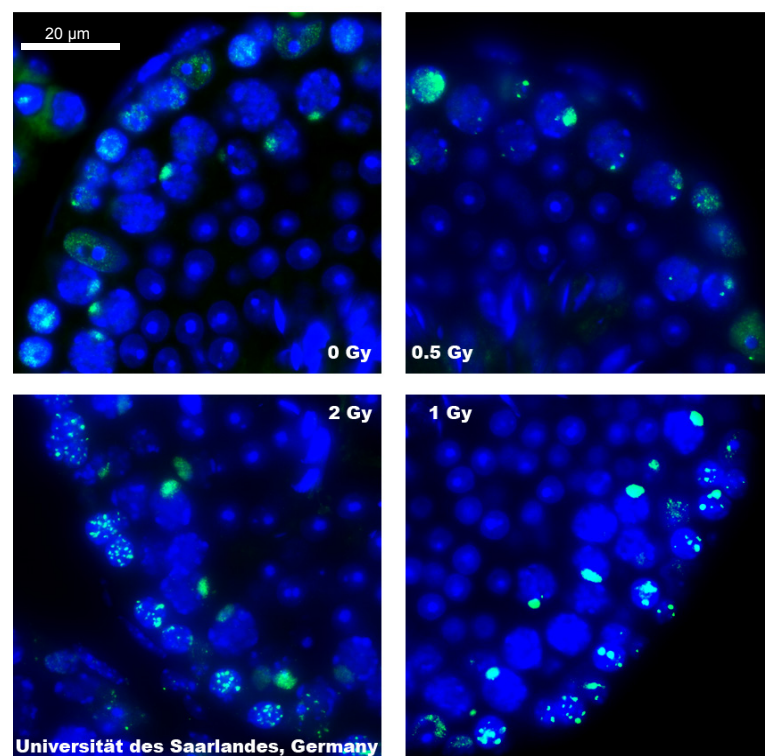
γ H2AX**53BP1**

Figure 13: Immunofluorescence stainings of γ -H2AX (upper panel) and 53BP1 (lower panel) in testis reveal the expression of these two repair proteins differs in different types of germ cell. 30 min after irradiation with 0.1 Gy, 0.5 Gy and 1.0 Gy, clear γ -H2AX foci appeared in round spermatids, while 53BP1 foci appeared in SSCs. The number of γ -H2AX and 53BP1 foci clearly increased with the increasing radiation doses in both analyzed types of germ cell.

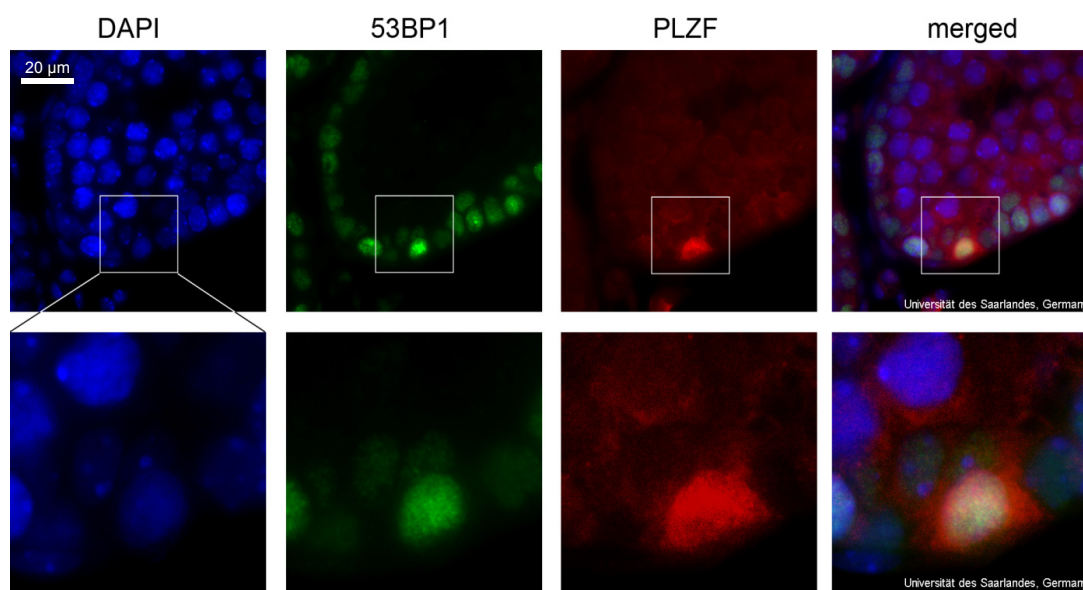


Figure 14: Immunofluorescence staining of PLZF/53BP1 double staining in testis shows that PLZF-positive (red) undifferentiated spermatogonia exhibited a kind of uniform pale nuclear staining with DAPI (blue) and strong basal staining for 53BP1 (green).

4.4. DSB induction in testis

Our data obtained by immunofluorescence staining indicate that 53BP1 and γ -H2AX were both expressed in the differentiated cells of lung and kidney, but their expression differed in the various subtypes of germ cells after irradiation (Fig. 13). Only 53BP1 foci were detected in undifferentiated PLZF-positive spermatogonia, while γ -H2AX foci appeared in PLZF-negative spermatogonia, spermatocytes and round spermatids. These findings strongly suggest that the DSB induction and rejoining in male germ cells may not be in line with those established in somatic cells.

To analyze the correlation between the number of foci and the irradiation dose in SSCs and round spermatids, we respectively counted 53BP1 or γ -H2AX foci at 30 min after irradiation with 0.1 Gy, 0.5 Gy and 1 Gy, and found that the foci formation was linearly dependent on the radiation dose in both germ cell types. However, the absolute yields of foci in each type were not identical with the

differentiated somatic cells analyzed. In SSCs, the foci yields (≈ 1 foci/cell after 0.1 Gy, ≈ 3.5 foci/cell after 0.5 Gy, and ≈ 5 foci/cell after 1 Gy) were slightly lower than the yields in differentiated somatic cells (Fig. 10). In haploid round spermatids, the expected yields of foci were close to one-half of the yields in diploid somatic cells on the basis of the half of DNA content. However, the actual foci yields were approximately the same as in differentiated somatic cells (≈ 5 foci/cell after 0.5 Gy, and ≈ 7 foci/cell after 1 Gy).

Despite the differences in the absolute foci yields, we observed a linear correlation between the foci number and the radiation dose in both types of germ cells. This enables us to compare the DSB repair kinetics between SSCs, round spermatids and differentiated somatic cells by using the same DSB repair marker.

4.5. DSB kinetics in germ cells

As shown in Fig. 12, at 5h post-irradiation, a highly increased γ -H2AX foci level (4.5 foci/cell) was found in round spermatids, whereas only 2 foci/cell was observed in the differentiated somatic cells. Moreover, round spermatids also exhibited significantly increased residual foci levels at 24h and 48h post-irradiation (2 foci/cell and 1.5 foci/cell), while only 0.5 foci/cell at 24h and 0.3 foci/cell at 48h were observed in the differentiated somatic cells. Obviously, the elimination of radiation-induced γ -H2AX foci in round spermatids was remarkably slower than that in somatic cells.

In contrast to round spermatids, the DSB repair kinetics of undifferentiated spermatogonia was generally similar to differentiated somatic cells, although moderate increased residual 53BP1 foci levels (11% at 24 h and 7% at 48 h in SSCs *versus* 6% at 24 h and 4% at 48 h in differentiated somatic cells) were observed at 24 h and 48 h post-irradiation (Fig. 11). Taken together, both analyzed germ cell

types displayed high residual foci levels, which suggest that the DSB repair in male germ cells is generally less efficient than in differentiated somatic cells. On the other hand, compared with differentiated round spermatids, undifferentiated spermatogonia definitely possess higher efficiencies in DSB repair.

5. Discussion

5.1 DSB induction in mouse testis

In the present study, we were able to distinguish undifferentiated spermatogonia from other subtypes of germ cells by PLZF immunofluorescence staining. The undifferentiated spermatogonia exhibited a kind of uniform pale nuclear staining with DAPI, known to be associated with lack of heterochromatin. By the high-resolution light microscopy and transmission electron microscopy, Chiarini-Garcia and Garcia observed that highly dense and moderately dense flecks of facultative heterochromatin are diffusely distributed throughout the nuclei of undifferentiated spermatogonia, leading to a mottled appearance. These flecks vanish in the following differentiating spermatogonia (A1-A4), and are replaced by the increasing heterochromatin masses along the nuclear envelope (Chiarini-Garcia and Russel, 2001; Chiarini-Garcia and Russel, 2002). It has been reported that chromatin structure may strongly influence the formation of γ -H2AX foci (Bewersdorf *et al.*, 2006; Cowell *et al.*, 2007; Goodarzi *et al.*; 2009). Blanco-Rodríguez observed that the levels of H2AX phosphorylation progressively increase with the gradually increasing amounts of heterochromatin in spermatogonia (Blanco-Rodríguez, 2009). Therefore, in the present study, the absence of γ -H2AX foci in PLZF-positive spermatogonia might be partly due to the distinct distribution of facultative heterochromatin in undifferentiated spermatogonia. Besides, we noticed that the background staining of 53BP1 in PLZF-positive spermatogonia was noticeably stronger than in differentiated somatic cells. This finding may also be associated with their distinct chromatin structure, and may probably affect the detection of some tiny 53BP1 foci, which might be one of the reasons for our finding of lower 53BP1 foci levels in the PLZF-positive spermatogonia compared to the differentiated somatic cells.

In contrast to undifferentiated spermatogonia, bright and clear γ -H2AX foci were detected in round spermatids after irradiation. Besides, in some given spermatogenic stages, round spermatids regularly exhibited some tiny speckle-like γ -H2AX foci. Recent studies have revealed that these foci are mainly located in the heterochromatin and are associated with the spontaneous occurrence of endogenous DSBs in the process of chromatin remodeling during the earlier stages of spermiogenesis (Marcon and Boissonneault, 2004; Leduc *et al.*, 2008). It should be noted that the spontaneous foci were significantly weaker and smaller than the irradiation-induced foci in round spermatids. Therefore, the spontaneous foci should not have interfered with our counting of radiation-induced γ -H2AX foci.

Due to their haploid DNA content, the yields of γ -H2AX foci in round spermatids were supposed to be close to one-half of yields of diploid cells, analyzed under same irradiation conditions. However, the actual mean value of γ -H2AX foci in round spermatids was approximately the same as that in differentiated somatic cells. The previous work of our laboratory has shown that the number of γ -H2AX foci formed in murine blood lymphocytes after irradiation with 2Gy is about 23 foci/cell at 5 min post-irradiation, and decreases to 12 foci/cell at 30 min post-irradiation (Rübe *et al.*, 2008a), suggesting that the number of γ -H2AX foci may reach peak values within 30 min after irradiation and then gradually diminishes with time. Therefore, in the present study, the high levels of γ -H2AX foci at 30 min post-irradiation may reflect the fact that the DSB repair in round spermatids is remarkably delayed compared with differentiated somatic cells, even before 30 min post-irradiation.

5.2 DSB repair in differentiated round spermatids

Upon exposure to radiation, eukaryotic cells repair DSBs primarily by two

pathways: HR and NHEJ (Jeggo, 1998; Johnson and Jasin, 2000). HR needs the undamaged sister chromatid as a template, thus particularly occurs in proliferative phase (Johnson and Jasin, 2000; Rothkamm and Löbrich, 2003), while NHEJ is active throughout the cell cycle and contributes to the repair of most DSBs in G1/G0 phase (Rothkamm *et al.*, 2003; Aylon and Kupiec, 2005). Therefore, differentiated somatic cells and haploid round spermatids are expected to repair DSBs by NHEJ rather than HR. Recent work from our laboratory has shown that differentiated somatic cells derived from different normal tissues have nearly identical DSB rejoining kinetics analyzed by enumerating γ -H2AX and 53BP1 foci in repair-proficient mice (Rübe *et al.*, 2008b). In the present study, however, 53BP1 was absent in round spermatids, and significantly increased γ -H2AX foci levels were observed at 5 h, 24 h and 48 h post-irradiation, suggesting that DSB repair in round spermatids is clearly less efficient and may differ from the classic NHEJ pathway established in differentiated somatic cells.

In differentiated somatic cells, the majority of radiation-induced DSBs are rejoining dominantly by NHEJ in a DNA-PK-dependent manner (Mahaney *et al.*, 2009). DNA-PK has been confirmed to play a major role in regulating the efficiency of NHEJ. Analysis of DSB rejoining in DNA-PK-proficient cells by pulsed-field gel electrophoresis has shown that DNA-PK-dependent NHEJ is a very fast process operating with half-times of 10-30 min after irradiation. Cells lacking the catalytic subunit of DNA-PK (or in which DNA-PKcs activity has been inhibited) are hypersensitive to radiation, showing an obviously slow rejoining of DSBs with a half time of 10-12 h (DiBiase *et al.*, 2000). Moreover, severe combined immunodeficiency (SCID) mice, characterized by a spontaneous mutation in the DNA-PKcs, exhibit strikingly increased residual foci levels after irradiation (50% at 5 h, 40% at 24 and 48 h) in differentiated somatic cells (Rübe *et al.*, in press). In addition, recent immunohistochemical studies have shown that DNA-PKcs is not

expressed in round spermatids (Hamer *et al.*, 2003), implying that the low efficacy of DSB rejoining of round spermatids is, at least in part, due to the lack of DNA-PK.

Whenever the activity of DNA-PK is compromised, DNA-PK-independent NHEJ may play an enhanced role in eliminating DSBs with slower kinetics (Perrault *et al.*, 2004). DNA-PK-independent NHEJ includes several different pathways and involves different associations of DNA repair proteins. Iwabuchi *et al.* demonstrated that 53BP1 can directly interact with LigIV/XRCC4 complex as a backup NHEJ pathway to rejoin DSBs in G1 phase cells when upstream phosphorylation signals are weak or absent (Iwabuchi *et al.*, 2003; Iwabuchi *et al.*, 2006). Besides, ATM, another member of PIKKs, was reported to contribute to DSB repair by an ATM-Artemis-LigIV/XRCC4-dependent pathway. This pathway is specifically required for repair of DSBs located close to or within heterochromatic regions, and needs the participation of other DDR-mediator proteins including 53BP1 (Goodarzi *et al.*, 2008; Kobayashi *et al.*, 2008; Goodarzi *et al.*, 2009). Therefore, the absence of 53BP1 may be another reason for the less efficient DSB repair in round spermatids.

Recently, a Lig IV/XRCC4-independent NHEJ pathway, termed 'B-NHEJ', was summarized by Iliakis (Iliakis, 2009). This pathway requires a set of proteins involved in DNA excision repair, such as Ligase III, Poly(ADP-ribose) Polymerase-1 and histone H1, and may function throughout the cell cycle with slower kinetics of several hours (Audebert *et al.*, 2006). DNA excision repair is an important pathway, mainly for the repair of DNA single-strand breaks (SSBs), but it also can be used for rejoining DSBs as a complementary mechanism. Recent studies have revealed that DNA excision repair is highly active in spermatids at the early stages of spermiogenesis (Olsen *et al.*, 2005), suggesting that 'B-NHEJ' may function in the DSB repair of round spermatids. It should be mentioned that the DSB rejoining by 'B-NHEJ' relies on the synapsis by random encounters of freely diffusing DNA ends, and thus often results in more extensive DNA deletions relative to D-NHEJ. This

might explain the increased incidence of chromosomal aberrations in spermatids after exposure to radiation (Iliakis *et al.*, 2007).

5.3 DSB repair in undifferentiated spermatogonia

In the seminiferous epithelium of adult mouse testis, the proliferative activity of SSCs follows a cyclic pattern (*i.e.* periods of quiescence followed by the active proliferation). Therefore, SSCs are mostly quiescent (G0 phase) during a particular period of each seminiferous epithelium cycle (de Rooij, 2001). Within a seminiferous epithelium cycle, the total duration of cell cycle in SSCs has been calculated to be in the range of about 70–100h, within which the actively proliferative phase last for about 40 h (de Rooij *et al.*, 2000). On the basis of these, we can infer that most of SSCs (estimated to be about 80%) do not divide (*i.e.* stay in G0/G1 phase) at any time, and thus the majority of SSCs analyzed in the present study are supposed to repair DSBs by NHEJ. Ahmed *et al.* recently analyzed the DSB repair in spermatogonia by immunofluorescence staining with antibodies against γ -H2AX and 53BP1, and found 60% residual foci levels for both markers at 16 h post-irradiation, suggesting a much slower and incomplete repair in spermatogonia compared with somatic cells. This less efficient DSB repair might be due to the absence of MDC1, an important DSB repair protein involved in the early signal amplification of DNA damage (Ahmed *et al.*, 2008). However, in the present study, we found that undifferentiated spermatogonia, a distinct subtype containing SSCs, were definitely negative for γ -H2AX staining, implying that the spermatogonia analyzed by Ahmed *et al.* should belong to differentiating spermatogonia subtypes. After enumerating 53BP1 foci, we found that the DSB rejoining kinetics of undifferentiated spermatogonia was generally similar to that of differentiated somatic cells in lung and kidney, although moderate increased residual foci levels were observed at late

time points (30% of foci levels at 5 h, 11% at 24 h and 7% at 48 h). Moreover, compared with differentiated spermatids, DSB repair in undifferentiated spermatogonia was undoubtedly proficient.

Spermatogonia are a heterogeneous population. It has been reported that differentiating spermatogonia (A1 to A4, In, and B spermatogonial cells) are most sensitive to killing by irradiation, whereas undifferentiated spermatogonia are moderate sensitivity to radiation (van der Meer *et al.*, 1992a; van der Meer *et al.*, 1992b; van der Meer *et al.*, 1993; Ogilvy-Stuart and Shalet, 1993; Judas *et al.*, 1996; Zhang *et al.*, 2007). Compared with the DSB repair in differentiating spermatogonia reported by Ahmed *et al.*, the DSB repair in undifferentiated spermatogonia analyzed in our experiment is quite efficient, although the different radiation dose was used (Ahmed *et al.*, 2008). Therefore, the different radiosensitivities between undifferentiated spermatogonia and differentiating spermatogonia may be partly explained by their different DSB repair efficiencies. On the other hand, differentiated somatic cells usually are thought to be relatively resistant to radiation. The discrepancy in DSB repair efficiency between undifferentiated spermatogonia and differentiated somatic cells seems not to explain fully the significant difference in the radiosensitivities between them, and thus other mechanisms may be operative.

The DSBs induced by radiation lead to a series of cellular responses such as cell-cycle arrest, DSB repair and apoptosis (Kastan and Bartek, 2004). Although DSB repair is a critical mechanism for maintaining genome stability in all cell types, the relative ability and even necessity to repair DSBs may vary depending on the specific cell type and developmental stage, and may change along the life time. As a result, distinct cell types at different developmental stages might adopt different cellular responses to counteract the deleterious effects of DSBs. While differentiated somatic cells senesce and die each generation, spermatogonia are responsible for faithfully transmitting genetic information from one generation to the next, and thus

must have more strict response mechanisms to repair DSBs and/or to eliminate damaged cells. It has been reported that the number of male germ cells at different developmental phases is regulated by a dynamic balance between cell proliferation and apoptosis (Tripathi *et al.*, 2009). Radiation-induced apoptosis of male germ cells primarily occurs in proliferating spermatogonia (Hasegawa *et al.*, 1997). Therefore, apoptosis as a main response to DNA damage may contribute to the elimination of damaged spermatogonia, leading to a higher radiosensitivity of spermatogonia compared with differentiated somatic cells. Further studies are required to elucidate the exact mechanism underlying this process.

6. References

1. **Ahmed EA, van der Vaart A, Barten A, Kal HB, Chen J, Lou Z, Minter-Dykhouse K, Bartkova J, Bartek J, de Boer P, de Rooij DG.** (2007) Differences in DNA double strand breaks repair in male germ cell types: lessons learned from a differential expression of Mdc1 and 53BP1. *DNA Repair*; 6(9): 1243-1254.
2. **Alberts B.** (2003) DNA replication and recombination. *Nature*; 421(6921): 431-435.
3. **Andegeko Y, Moyal L, Mittelman L, Tsarfaty I, Shiloh Y, Rotman G.** (2001) Nuclear retention of ATM at sites of DNA double strand breaks. *J Biol Chem*; 276(41): 38224–38230.
4. **Anderson L, Henderson C, Adachi Y.** (2001) Phosphorylation and rapid relocalization of 53BP1 to nuclear foci upon DNA damage. *Mol Cell Biol*; 21(5): 1719–1729.
5. **Audebert M, Salles B, Weinfeld M, Calsou P.** (2006) Involvement of polynucleotide kinase in a poly (ADP-ribose) polymerase-1-dependent DNA double-strand breaks rejoining pathway. *J Mol Biol*; 356(2): 257-265.
6. **Aylon Y, Kupiec M.** (2005) Cell cycle-dependent regulation of double-strand break repair: a role for the CDK. *Cell Cycle*; 4(2): 259-261.
7. **Bassing CH, Chua KF, Sekiguchi J, Suh H, Whitlow SR, Fleming JC, Monroe BC, Ciccone DN, Yan C, Vlasakova K, Livingston DM, Ferguson DO, Scully R, Alt FW.** (2002) Increased ionizing radiation sensitivity and genomic instability in the absence of histone H2AX. *Proc Natl Acad Sci*; 99(12): 8173-8178.
8. **Bekker-Jensen S, Lukas C, Melander F, Bartek J, Lukas J.** (2005) Dynamic assembly and sustained retention of 53BP1 at the sites of DNA damage are controlled by Mdc1/NFBD1. *J Cell Biol*; 170(2): 201–211.
9. **Bekker-Jensen S, Lukas C, Kitagawa R, Melander F, Kastan MB, Bartek J, Lukas J.** (2006) Spatial organization of the mammalian genome surveillance machinery in response to DNA strand breaks. *J Cell Biol*; 173(2): 195-206.

10. **Bewersdorf J, Bennett BT, Knight KL.** (2006) H2AX chromatin structures and their response to DNA damage revealed by 4Pi microscopy. *Proc Natl Acad Sci*; 103(48): 18137-18142.
11. **Bhogal N, Jalali F, Bristow RG.** (2009) Microscopic imaging of DNA repair foci in irradiated normal tissues. *Int J Radiat Biol*; 85(9): 732-746.
12. **Blanco-Rodríguez J.** (2009) gammaH2AX marks the main events of the spermatogenic process. *Microsc Res Tech*; 72(11): 823-832.
13. **Brewer L, Corzett M, Balhorn R.** (2002) Condensation of DNA by spermatid basic nuclear proteins. *J Biol Chem*; 277(41): 38895–38900.
14. **Brinster RL, Avarbock MR.** (1994) Germline transmission of donor haplotype following spermatogonial transplantation. *Proc Natl Acad Sci*; 91(24): 11303–11307.
15. **Brinster RL, Zimmermann JW.** (1994) Spermatogenesis following male germ-cell transplantation. *Proc Natl Acad Sci*; 91(24): 11298–11302.
16. **Brinster RL.** (2002). Germline stem cell transplantation and transgenesis. *Science*; 296(5576): 2174–2176.
17. **Buaas FW, Kirsh AL, Sharma M, McLean DJ, Morris JL, Griswold MD, de Rooij DG, Braun RE.** (2004) Plzf is required in adult male germ cells for stem cell self-renewal. *Nat Genet*; 36(6): 647-652.
18. **Burma S, Chen BP, Murphy M, Kurimasa A, Chen DJ.** (2001) ATM phosphorylates histone H2AX in response to DNA double-strand breaks. *J Biol Chem*; 276(45): 42462–42467.
19. **Carrell DT, Emery BR, Hammoud S.** (2007) Altered protamine expression and diminished spermatogenesis: what is the link? *Hum Reprod Update*; 13(3): 313-327.
20. **Celeste A, Petersen S, Romanienko PJ, Fernandez-Capetillo O, Chen HT, Sedelnikova OA, Reina-San-Martin B, Coppola V, Meffre E, Difilippantonio MJ, Redon C, Pilch DR, Oлару A, Eckhaus M, Camerini-Otero RD, Tessarollo L, Livak F, Manova K, Bonner WM, Nussenzweig MC, Nussenzweig A.** (2002) Genomic instability in mice

lacking histone H2AX. *Science*; 296(5569): 922-927.

21. **Celeste A, Fernandez-Capetillo O, Kruhlak MJ, Pilch DR, Staudt DW, Lee A, Bonner RF, Bonner WM, Nussenzweig A.** (2003) Histone H2AX phosphorylation is dispensable for the initial recognition of DNA breaks. *Nat Cell Biol*; 5(7): 675–679.
22. **Chiarini-Garcia H, Hornick JR, Griswold MD, Russell LD.** (2001) Distribution of type A spermatogonia in the mouse is not random. *Biol Reprod*; 65(4): 1179-1185.
23. **Chiarini-Garcia H, Russell LD.** (2001) High-resolution light microscopic characterization of mouse spermatogonia. *Biol Reprod*; 65(4):1170-1178.
24. **Chiarini-Garcia H, Russell LD.** (2002) Characterization of mouse spermatogonia by transmission electron microscopy. *Reproduction*; 123(4): 567-577.
25. **Chiarini-Garcia H, Raymer AM, Russell LD.** (2003) Non-random distribution of spermatogonia in rats: evidence of niches in the seminiferous tubules. *Reproduction*; 126(5): 669-680.
26. **Chicheportiche A, Bernardino-Sgherri J, de Massy B, Dutrillaux B.** (2007) Characterization of Spo11-dependent and independent phospho-H2AX foci during meiotic prophase I in the male mouse. *J Cell Sci*; 120: 1733-1742.
27. **Costantini S, Woodbine L, Andreoli L, Jeggo PA, Vindigni A.** (2007) Interaction of the Ku heterodimer with the DNA ligase IV/Xrcc4 complex and its regulation by DNA-PK. *DNA Repair*; 6(6): 712–722.
28. **Costoya JA, Hobbs RM, Barna M, Cattoretti G, Manova K, Sukhwani M, Orwig KE, Wolgemuth DJ, Pandolfi PP.** (2004) Essential role of Plzf in maintenance of spermatogonial stem cells. *Nat Genet*; 36(6): 653-659.
29. **Cowell IG, Sunter NJ, Singh PB, Austin CA, Durkacz BW, Tilby MJ.** (2007) gammaH2AX foci form preferentially in euchromatin after ionising-radiation. *PLoS One*; 2(10): e1057.
30. **de Rooij DG.** (1973) Spermatogonial stem cell renewal in the mouse. I. Normal situation. *Cell Tissue Kinet*; 6(3): 281–287.

31. **de Rooij DG, Russell LD.** (2000) All you wanted to know about spermatogonia but were afraid to ask. *J Androl*; 21(6): 776-798.
32. **de Rooij DG.** (2001) Proliferation and differentiation of spermatogonial stem cells. *Reproduction*; 121(3): 347-354.
33. **de Rooij DG.** (2009) The spermatogonial stem cell niche. *Microsc Res Tech*; 72(8): 580-585.
34. **DiBiase SJ, Zeng ZC, Chen R, Hyslop T, Curran WJ Jr, Iliakis G.** (2000) DNA-dependent protein kinase stimulates an independently active, nonhomologous, end-joining apparatus. *Cancer Res*; 60(5): 1245-1253.
35. **Dym M, Fawcett DW.** (1970) The blood-testis barrier in the rat and the physiological compartmentation of the seminiferous epithelium. *Biol Reprod*; 3(3): 308-326.
36. **Ehmcke J, Wistuba J, Schlatt S.** (2006) Spermatogonial stem cells: questions, models and perspectives. *Hum Reprod Update*; 12(3): 275-282.
37. **Eliezer Y, Argaman L, Rhie A, Doherty AJ, Goldberg M.** (2009) The direct interaction between 53BP1 and MDC1 is required for the recruitment of 53PB1 to sites of damage. *J Biol Chem*; 284(1): 426-435.
38. **Fernandez-Capetillo O, Celeste A, Nussenzweig A.** (2003) Focusing on foci: H2AX and the recruitment of DNA-damage response factors. *Cell Cycle*; 2(5): 426-427.
39. **Fernandez-Capetillo O, Lee A, Nussenzweig M, Nussenzweig A.** (2004) H2AX: the histone guardian of the genome. *DNA Repair*; 3(8-9): 959-967.
40. **Filipponi D, Hobbs RM, Ottolenghi S, Rossi P, Jannini EA, Pandolfi PP, Dolci S.** (2007) Repression of kit expression by Plzf in germ cells. *Mol Cell Biol*; 27(19): 6770-6781.
41. **Fillingham J, Keogh MC, Krogan NJ.** (2006) GammaH2AX and its role in DNA double-strand break repair. *Biochem Cell Biol*; 84(4): 568-577.
42. **Fitzgerald JE, Grenon M, Lowndes NF.** (2009) 53BP1: function and mechanisms of focal recruitment. *Biochem Soc Trans*; 37: 897-904.

43. **Furuta T, Takemura H, Liao ZY, Aune GJ, Redon C, Sedelnikova OA, Pilch DR, Rogakou EP, Celeste A, Chen HT, Nussenzweig A, Aladjem MI, Bonner WM, Pommier Y.** (2003) Phosphorylation of histone H2AX and activation of Mre11, Rad50, and Nbs1 in response to replication-dependent DNA double-strand breaks induced by mammalian DNA topoisomerase I cleavage complexes. *J Biol Chem*; 278(22): 20303-20312.
44. **Gao Y, Chaudhuri J, Zhu C, Davidson L, Weaver DT, Alt FW.** (1998) A targeted DNA-PKcs-null mutation reveals DNA-PK-independent functions for KU in V(D)J recombination. *Immunity*; 9(3): 367-376.
45. **Gellert M.** (2002) V(D)J recombination: RAG proteins, repair factors, and regulation. *Annu Rev Biochem*; 71: 101-132.
46. **Goedecke W, Eijpe M, Offenbergh HH, van Aalderen M, Heyting C.** (1999) Mre11 and Ku70 interact in somatic cells, but are differentially expressed in early meiosis. *Nat Genet*; 23(2): 194–198.
47. **Goodarzi AA, Noon AT, Deckbar D, Ziv Y, Shiloh Y, Löbrich M, Jeggo PA.** (2008) ATM signaling facilitates repair of DNA double-strand breaks associated with heterochromatin. *Mol Cell*; 31(2): 167–177.
48. **Goodarzi AA, Noon AT, Jeggo PA.** (2009) The impact of heterochromatin on DSB repair. *Biochem Soc Trans*; 37: 569-576.
49. **Gu Y, Jin S, Gao Y, Weaver DT, Alt FW.** (1997) Ku70-deficient embryonic stem cells have increased ionizing radiosensitivity, defective DNA end-binding activity, and inability to support V(D)J recombination. *Proc Natl Acad Sci U S A*; 94(15): 8076-8081.
50. **Hamasaki K, Imai K, Nakachi K, Takahashi N, Kodama Y, Kusunoki Y.** (2007) Short-term culture and gammaH2AX flow cytometry determine differences in individual radiosensitivity in human peripheral T lymphocytes. *Environ Mol Mutagen*; 48(1): 38–47.
51. **Hamer G, Roepers-Gajadien HL, van Duyn-Goedhart A, Gademan IS, Kal HB, van Buul PP, Ashley T, de Rooij DG.** (2003) Function of DNA-protein kinase catalytic subunit during the early meiotic prophase without Ku70 and Ku86. *Biol Reprod*; 68(3): 717-721.
52. **Hasegawa M, Wilson G, Russell LD, Meistrich ML.** (1997)

Radiation-induced cell death in the mouse testis: relationship to apoptosis. *Radiat Res*; 147(4): 457-467.

53. **Hoeijmakers JH.** (2001) Genome maintenance mechanisms for preventing cancer. *Nature*; 411(6835): 366–374.
54. **Iliakis G, Wenqi W, Minli W, Georgia I. Terzoudi, Gabriel E. Pantelias.** (2007) Backup pathways of nonhomologous end joining may have a dominant role in the formation of chromosome aberrations. *Chromosomal Alterations Methods, Results and Importance in Human Health*; Springer Berlin Heidelberg: 67-85.
55. **Iliakis G.** (2009) Backup pathways of NHEJ in cells of higher eukaryotes: cell cycle dependence. *Radiother Oncol*; 92(3): 310-315.
56. **Iwabuchi K, Basu BP, Kysela B, Kurihara T, Shibata M, Guan D, Cao Y, Hamada T, Imamura K, Jeggo PA, Date T, Doherty AJ.** (2003) Potential role for 53BP1 in DNA end-joining repair through direct interaction with DNA. *J Biol Chem*; 278(38): 36487–36495.
57. **Iwabuchi K, Hashimoto M, Matsui T, Kurihara T, Shimizu H, Adachi N, Ishiai M, Yamamoto K, Tauchi H, Takata M, Koyama H, Date T.** (2006) 53BP1 contributes to survival of cells irradiated with X-ray during G1 without Ku70 or Artemis. *Genes Cells*; 11(8): 935-948.
58. **Jeggo PA.** (1998) DNA breakage and repair. *Adv Genet*; 38: 185–218.
59. **Johnson RD, Jasin M.** (2000) Sister chromatid gene conversion is a prominent double-strand break repair pathway in mammalian cells. *EMBO J*; 19(13): 3398–3407.
60. **Judas L, Bentzen SM, Hansen PV, Overgaard J.** (1996) Proliferative response of mouse spermatogonial stem cells after irradiation: a quantitative model analysis of experimental data. *Cell Prolif*; 29(2): 73-87.
61. **Kastan MB, Bartek J.** (2004) Cell-cycle checkpoints and cancer. *Nature*; 432(7015): 316–323.
62. **Kobayashi J, Iwabuchi K, Miyagawa K, Sonoda E, Suzuki K, Takata M, Tauchi H.** (2008) Current topics in DNA double-strand break repair. *J Radiat Res*; 49(2): 93-103.

63. **Leduc F, Maquennehan V, Nkoma GB, Boissonneault G.** (2008) DNA damage response during chromatin remodeling in elongating spermatids of mice. *Biol Reprod*; 78(2): 324-332.
64. **Lees-Miller SP, Meek K.** (2003) Repair of DNA double strand breaks by non-homologous end joining. *Biochimie*; 85(11): 1161-1173.
65. **Li L, Xie T.** (2005) Stem cell niche: structure and function. *Annu Rev Cell Dev Biol*; 21: 605–631.
66. **Li L, Zou L.** (2005) Sensing, signaling, and responding to DNA damage: organization of the checkpoint pathways in mammalian cells. *J Cell Biochem*; 94(2): 298–306.
67. **Li W, Ma H.** (2006) Double-stranded DNA breaks and gene functions in recombination and meiosis. *Cell Res*; 16(5): 402-412.
68. **Lieber MR, Ma Y, Pannicke U, Schwarz K.** (2004) The mechanism of vertebrate nonhomologous DNA end joining and its role in V(D)J recombination. *DNA Repair*; 3(8-9): 817-826.
69. **Liu SK, Olive PL, Bristow RG.** (2008) Biomarkers for DNA DSB inhibitors and radiotherapy clinical trials. *Cancer Metastasis Rev*; 27(3): 445–458.
70. **Lou Z, Chini CC, Minter-Dykhouse K, Chen J.** (2003) Mediator of DNA damage checkpoint protein 1 regulates BRCA1 localization and phosphorylation in DNA damage checkpoint control. *J Biol Chem*; 278(16): 13599-13602.
71. **Lou Z, Chen BP, Asaithamby A, Minter-Dykhouse K, Chen DJ, Chen J.** (2004) MDC1 regulates DNA-PK autophosphorylation in response to DNA damage. *J Biol Chem*; 279(45): 46359-46362.
72. **Lou Z, Minter-Dykhouse K, Franco S, Gostissa M, Rivera MA, Celeste A, Manis JP, van Deursen J, Nussenzweig A, Paull TT, Alt FW, Chen J.** (2006) MDC1 maintains genomic stability by participating in the amplification of ATM-dependent DNA damage signals. *Mol Cell*; 21(2): 187–200.
73. **Mahaney BL, Meek K, Lees-Miller SP.** (2009) Repair of ionizing radiation-induced DNA double-strand breaks by non-homologous end-joining.

Biochem J; 417(3): 639-650.

74. **Marchetti F, Coleman MA, Jones IM, Wyrobek AJ.** (2006) Candidate protein biosimeters of human exposure to ionizing radiation. *Int J Radiat Biol*; 82(9): 605–639.
75. **Marcon L, Boissonneault G.** (2004) Transient DNA strand breaks during mouse and human spermiogenesis new insights in stage specificity and link to chromatin remodeling. *Biol Reprod*; 70(4): 910-918.
76. **Meng X, Lindahl M, Hyvönen ME, Parvinen M, de Rooij DG, Hess MW, Raatikainen-Ahokas A, Sainio K, Rauvala H, Lakso M, Pichel JG, Westphal H, Saarma M, Sariola H.** (2000) Regulation of cell fate decision of undifferentiated spermatogonia by GDNF. *Science*; 287(5457): 1489-1493.
77. **Meng X, de Rooij DG, Westerdahl K, Saarma M, Sariola H.** (2001) Promotion of seminomatous tumors by targeted overexpression of glial cell line-derived neurotrophic factor in mouse testis. *Cancer Res*; 61(8): 3267-3271.
78. **Mochan TA, Venere M, DiTullio RA Jr, Halazonetis TD.** (2004) 53BP1, an activator of ATM in response to DNA damage. *DNA Repair*; 3(8-9):945-52.
79. **Morgan WF, Corcoran J, Hartmann A, Kaplan MI, Limoli CL, Ponnaiya B.** (1998) DNA double-strand breaks, chromosomal rearrangements, and genomic instability. *Mutat Res*; 404(1-2): 125–128.
80. **Nakada S, Chen GI, Gingras AC, Durocher D.** (2008) PP4 is a gammaH2AX phosphatase required for recovery from the DNA damage checkpoint. *EMBO Rep* 9(10): 1019–1026.
81. **Nakamura K, Sakai W, Kawamoto T, Bree RT, Lowndes NF, Takeda S, Taniguchi Y.** (2006) Genetic dissection of vertebrate 53BP1: a major role in non-homologous end joining of DNA double strand breaks. *DNA Repair*; 5(6): 741–749.
82. **Nazarov IB, Smirnova AN, Krutilina RI, Svetlova MP, Solovjeva LV, Nikiforov AA, Oei SL, Zalenskaya IA, Yau PM, Bradbury EM, Tomilin NV.** (2003) Dephosphorylation of histone gamma-H2AX during repair of DNA double-strand breaks in mammalian cells and its inhibition by calyculin A. *Radiat Res*; 160(3): 309-317

83. **Nussenzweig A, Chen C, da Costa Soares V, Sanchez M, Sokol K, Nussenzweig MC, Li GC.** (1996) Requirement for Ku80 in growth and immunoglobulin V(D)J recombination. *Nature*; 382(6591): 551-555.
84. **Nussenzweig A, Sokol K, Burgman P, Li L, Li GC.** (1997) Hypersensitivity of Ku80-deficient cell lines and mice to DNA damage: the effects of ionizing radiation on growth, survival, and development. *Proc Natl Acad Sci*; 94(25): 13588-13593.
85. **Oakberg EF.** (1971) Spermatogonial stem-cell renewal in the mouse. *Anat Rec*; 169(3): 515-531.
86. **Oatley JM, Brinster RL.** (2006) Spermatogonial stem cells. *Methods Enzymol*; 419: 259-282.
87. **Ogilvy-Stuart AL, Shalet SM.** (1993) Effect of radiation on the human reproductive system. *Environ Health Perspect*; 101 (2 Suppl): 109-116.
88. **Olive PL.** (1998) The role of DNA single- and double-strand breaks in cell killing by ionizing radiation. *Radiat Res*; 150(5 Suppl): S42-51.
89. **Olive PL, Banáth JP.** (2004) Phosphorylation of histone H2AX as a measure of radiosensitivity. *Int J Radiat Oncol Biol Phys*; 58(2): 331-335.
90. **Olsen AK, Lindeman B, Wiger R, Duale N, Brunborg G.** (2005) How do male germ cells handle DNA damage? *Toxicol Appl Pharmacol*; 207(2 Suppl): 521-531.
91. **Paull TT, Rogakou EP, Yamazaki V, Kirchgessner CU, Gellert M, Bonner WM.** (2000) A critical role for histone H2AX in recruitment of repair factors to nuclear foci after DNA damage. *Curr Biol*; 10(15): 886-895.
92. **Payne C, Braun RE.** (2006) Histone lysine trimethylation exhibits a distinct perinuclear distribution in Plzf-expressing spermatogonia. *Dev Biol*; 293(2): 461-472.
93. **Pellegrini L, Yu DS, Lo T, Anand S, Lee M, Blundell TL, Venkitaraman AR.** (2002) Insights into DNA recombination from the structure of a RAD51-BRCA2 complex. *Nature*; 420(6913): 287-293.
94. **Perrault R, Wang H, Wang M, Rosidi B, Iliakis G.** (2004) Backup pathways

of NHEJ are suppressed by DNA-PK. *J Cell Biochem*; 92(4): 781-794.

95. **Pilch DR, Sedelnikova OA, Redon C, Celeste A, Nussenzweig A, Bonner WM.** (2003) Characteristics of gamma-H2AX foci at DNA double-strand breaks sites. *Biochem Cell Biol*; 81(3): 123–129.
96. **Porcedda P, Turinetto V, Lantelme E, Fontanella E, Chrzanowska K, Ragona R, De Marchi M, Delia D, Giachino C.** (2006) Impaired elimination of DNA double-strand break-containing lymphocytes in ataxia telangiectasia and Nijmegen breakage syndrome. *DNA Repair*; 5(8): 904–913.
97. **Porcedda P, Turinetto V, Orlando L, Lantelme E, Brusco A, De Marchi M, Amoroso A, Ricardi U, Gregori D, Giachino C.** (2009) Two-tier analysis of histone H2AX phosphorylation allows the identification of Ataxia Telangiectasia heterozygotes. *Radiother Oncol*; 92(1): 133–137.
98. **Rappold I, Iwabuchi K, Date T, Chen J.** (2001) Tumor suppressor p53 binding protein (53BP1) is involved in DNA damage-signaling pathways. *J Cell Biol*; 153(3): 613–620.
99. **Redon C, Pilch D, Rogakou E, Sedelnikova O, Newrock K, Bonner W.** (2002) Histone H2A variants H2AX and H2AZ. *Curr Opin Genet Dev*; 12(2): 162–169.
100. **Reid A, Gould A, Brand N, Cook M, Strutt P, Li J, Licht J, Waxman S, Krumlauf R, Zelent A.** (1995) Leukemia translocation gene, PLZF, is expressed with a speckled nuclear pattern in early hematopoietic progenitors. *Blood*; 86(12): 4544-4552.
101. **Rogakou EP, Pilch DR, Orr AH, Ivanova VS, Bonner WM.** (1998) DNA double-stranded breaks induce histone H2AX phosphorylation on serine 139. *J Biol Chem*; 273(10): 5858–5868.
102. **Rogakou EP, Boon C, Redon C, Bonner WM.** (1999) Megabase chromatin domains involved in DNA double-strand breaks in vivo. *J Cell Biol*; 146(5): 905–916.
103. **Rooney S, Alt FW, Lombard D, Whitlow S, Eckersdorff M, Fleming J, Fugmann S, Ferguson DO, Schatz DG, Sekiguchi J.** (2003) Defective DNA repair and increased genomic instability in Artemis-deficient murine cells. *J Exp Med*; 197(5): 553-565.

104. **Rothkamm K, Krüger I, Thompson LH, Löbrich M.** (2003) Pathways of DNA double-strand break repair during the mammalian cell cycle. *Mol Cell Biol*; 23(16): 5706-5715.
105. **Rothkamm K, Löbrich M.** (2003) Evidence for a lack of DNA double-strand break repair in human cells exposed to very low x-ray doses. *Proc Natl Acad Sci U S A*; 100(9): 5057–5062.
106. **Rübe CE, Grudzenski S, Kühne M, Dong X, Rief N, Löbrich M, Rübe C.** (2008a) DNA double-strand break repair of blood lymphocytes and normal tissues analysed in a preclinical mouse model: implications for radiosensitivity testing. *Clin Cancer Res*; 14(20): 6546-6555.
107. **Rübe CE, Dong X, Kühne M, Fricke A, Kaestner L, Lipp P, Rübe C.** (2008b) DNA double-strand break rejoining in complex normal tissues. *Int J Radiat Oncol Biol Phys*; 72(4): 1180-1187.
108. **Rübe CE, Fricke A, Wendorf J, Stützel A, Kühne M, Ong MF, Lipp P, Rübe C.** Accumulation of DNA double-strand breaks in normal-tissues after fractionated irradiation. *Int J Radiat Oncol Biol Phys*; (in press)
109. **Rupnik A, Grenon M, Lowndes N.** (2008) The MRN complex. *Curr Biol*; 18(11): R455–457.
110. **San Filippo J, Sung P, Klein H.** (2008) Mechanism of eukaryotic homologous recombination. *Annu Rev Biochem*; 77: 229-257.
111. **Sariola H, Saarma M.** (2003) Novel functions and signalling pathways for GDNF. *J Cell Sci*; 116: 3855-3862.
112. **Schrans-Stassen BH, van de Kant HJ, de Rooij DG, van Pelt AM.** (1999) Differential expression of c-kit in mouse undifferentiated and differentiating type A spermatogonia. *Endocrinology*; 140(12): 5894–5900.
113. **Schultz LB, Chehab NH, Malikzay A, Halazonetis TD.** (2000) p53 Binding protein 1 (53BP1) is an early participant in the cellular response to DNA double-strand breaks. *J Cell Biol*; 151(7): 1381–1390.
114. **Sedelnikova OA, Pilch DR, Redon C, Bonner WM.** (2003) Histone H2AX in DNA damage and repair. *Cancer Biol Ther*; 2(3): 233–235.

115. **Shetty G, Meistrich ML.** (2007) The missing niche for spermatogonial stem cells: Do blood vessels point the way? *Cell Stem Cell*; 1(4): 361–363.
116. **Shrivastav M, De Haro LP, Nickoloff JA.** (2008) Regulation of DNA double-strand break repair pathway choice. *Cell Res*; 18(1): 134-147.
117. **Spradling A, Drummond-Barbosa D, Kai T.** (2001) Stem cells find their niche. *Nature*; 414(6859): 98-104.
118. **Stewart GS, Wang B, Bignell CR, Taylor AM, Elledge SJ.** (2003) MDC1 is a mediator of the mammalian DNA damage checkpoint. *Nature*; 421(6926): 961–966.
119. **Stiff T, O'Driscoll M, Rief N, Iwabuchi K, Löbrich M, Jeggo PA.** (2004) ATM and DNA-PK function redundantly to phosphorylate H2AX after exposure to ionizing radiation. *Cancer Res*; 64(7): 2390–2396.
120. **Stucki M, Clapperton JA, Mohammad D, Yaffe MB, Smerdon SJ, Jackson SP.** (2005) MDC1 directly binds phosphorylated histone H2AX to regulate cellular responses to DNA double-strand breaks. *Cell*; 123(7): 1213–1226.
121. **Stucki M, Jackson SP.** (2006) gammaH2AX and MDC1: anchoring the DNA-damage-response machinery to broken chromosomes. *DNA Repair*; 5(5): 534-543.
122. **Taccioli GE, Amatucci AG, Beamish HJ, Gell D, Xiang XH, Torres Arzayus MI, Priestley A, Jackson SP, Marshak Rothstein A, Jeggo PA, Herrera VL.** (1998) Targeted disruption of the catalytic subunit of the DNA-PK gene in mice confers severe combined immunodeficiency and radiosensitivity. *Immunity*; 9(3): 355-366.
123. **Tadokoro Y, Yomogida K, Ohta H, Tohda A, Nishimune Y.** (2002) Homeostatic regulation of germinal stem cell proliferation by the GDNF/FSH pathway. *Mech Dev*; 113(1): 29-39.
124. **Taneja N, Davis M, Choy JS, Beckett MA, Singh R, Kron SJ, Weichselbaum RR.** (2004) Histone H2AX phosphorylation as a predictor of radiosensitivity and target for radiotherapy. *J Biol Chem*; 279(3): 2273–2280.

125. **Tegelenbosch RA, de Rooij DG.** (1993) A quantitative study of spermatogonial multiplication and stem cell renewal in the C3H/101 F1 hybrid mouse. *Mutat Res*; 290(2): 193-200.
126. **Thompson LH, Schild D.** (2001) Homologous recombinational repair of DNA ensures mammalian chromosome stability. *Mutat Res*; 477(1-2): 131-153.
127. **Tichy ED, Stambrook PJ.** (2008) DNA repair in murine embryonic stem cells and differentiated cells. *Exp Cell Res*; 314(9): 1929-1936.
128. **Tripathi R, Mishra DP, Shaha C.** (2009) Male germ cell development: turning on the apoptotic pathways. *J Reprod Immunol*; 83(1-2): 31-35.
129. **Valerie K, Povirk LF.** (2003) Regulation and mechanisms of mammalian double-strand break repair. *Oncogene*; 22(37):5792-5812.
130. **van Gent DC, Hoeijmakers JH, Kanaar R.** (2001) Chromosomal stability and the DNA double-stranded break connection. *Nat Rev Genet*; 2(3): 196–206.
131. **van der Meer Y, Huiskamp R, Davids JA, van der Tweel I, de Rooij DG.** (1992a) The sensitivity of quiescent and proliferating mouse spermatogonial stem cells to X irradiation. *Radiat Res*; 130(3): 289-295.
132. **van der Meer Y, Huiskamp R, Davids JA, van der Tweel I, de Rooij DG.** (1992b) The sensitivity to X rays of mouse spermatogonia that are committed to differentiate and of differentiating spermatogonia. *Radiat Res*; 130(3): 296-302.
133. **van der Meer Y, Cattanach BM, de Rooij DG.** (1993) The radiosensitivity of spermatogonial stem cells in C3H/101 F1 hybrid mice. *Mutat Res*; 290(2): 201-210.
134. **Walker JR, Corpina RA, Goldberg J.** (2001) Structure of the Ku heterodimer bound to DNA and its implications for double-strand break repair. *Nature*; 412(6847): 607–614.
135. **Wang H, Wang M, Wang H, Böcker W, Iliakis G.** (2005) Complex H2AX phosphorylation patterns by multiple kinases including ATM and DNA-PK in human cells exposed to ionizing radiation and treated with kinase inhibitors. *J Cell Physiol*; 202(2): 492–502.

136. **Ward IM, Chen J.** (2001) Histone H2AX is phosphorylated in an ATR-dependent manner in response to replicational stress. *J Biol Chem*; 276(51): 47759–47762.
137. **Ward IM, Minn K, Jorda KG, Chen J.** (2003a) Accumulation of checkpoint protein 53BP1 at DNA breaks involves its binding to phosphorylated histone H2AX. *J Biol Chem*; 278(22): 19579–19582.
138. **Ward IM, Minn K, van Deursen J, Chen J.** (2003b) p53 binding protein 53BP1 is required for DNA damage responses and tumor suppression in mice. *Mol Cell Biol*; 23(7): 2556–2563.
139. **West SC.** (2003) Molecular views of recombination proteins and their control. *Nat Rev Mol Cell Biol*; 4(6): 435–445.
140. **Weterings E, van Gent DC.** (2004) The mechanism of non-homologous end-joining: a synopsis of synapsis. *DNA Repair*; 3(11): 1425-1435.
141. **Xu X, Stern DF.** (2003). NFB1/MDC1 regulates ionizing radiation induced focus formation by DNA checkpoint signaling and repair factors. *FASEB J*; 17(13): 1842-1848.
142. **Yoshida S, Sukeno M, Nabeshima Y.** (2007) A vasculature-associated niche for undifferentiated spermatogonia in the mouse testis. *Science*; 317(5845): 1722–1726.
143. **Yoshida S.** (2008) Spermatogenic stem cell system in the mouse testis. *Cold Spring Harb Symp Quant Biol*; 73:25-32.
144. **Zhang Z, Shao S, Meistrich ML.** (2007) The radiation-induced block in spermatogonial differentiation is due to damage to the somatic environment, not the germ cells. *J Cell Physiol*; 211(1): 149-158.
145. **Zhou BB, Elledge SJ.** (2000) The DNA damage response: putting checkpoints in perspective. *Nature*; 408(6811): 433–439.

Acknowledgements

During my stay in Homburg as a visiting doctor, I was very lucky to meet so many kind people who tried their best to help me. It is their help that I can accomplish the research project successfully.

First and foremost, I would like to express my thanks to Prof. Dr. Christian Rube for kindly offering me such a precious opportunity to work in his department and laboratory, giving me this thesis project. I am also very grateful to him for his kinds of support and concern.

At the same time, I would like to express my thanks to Priv.-Doz. Dr. Claudia E. Rube for her excellent direction and critical correcting of the manuscript as well as her generous helps in many aspects.

Also I am grateful to Dr. Andreas Fricke, Mrs. Nadine Miebach and Mrs. Daniela Ludwig in the laboratory of radiotherapy, who give a lot of help in my project. Special thanks go to Mr. Georg Blass and all the kind persons in radiotherapy room, they have given me too much help to finish this project.

At last I thank Prof. Dr. Gang Wu and Prof. Dr. Li Liu in Wuhan Union Hospital Cancer center, Tongji Medical College (China), for their kind support to my study in Germany.

Last but not least, I acknowledge my family financially and spiritually. They all tried their best to support me.

Curriculum Vitae

Name	Sheng Zhang
Date of Birth	Apr. 03, 1975
Place of birth	Wuhan, China
Sex:	Male
Nationality:	Chinese
Marital status:	Married
Address:	Cancer Center of Union Hospital, Wu Jia Dun District 56th, Hankou, Wuhan, 430023, P.R. China

Education and professional experience

1981 – 1987	Primary school in Wuhan, China
1987 – 1990	Junior school in Wuhan, China
1990 – 1993	Senior school in Wuhan, China
1993 – 1999	Tongji Medical University, Bachelor of Medicine, Wuhan, China
1999 – 2000	Department of Oncology, Zhongnan Hospital of Wuhan University, resident
2000 – 2002	Department of Oncology, Cancer Institute of China Academy of Medical Sciences, advanced training on Radiotherapy,
2002 – 2005	Union Hospital Cancer Center, Tongji Medical College, Huazhong Science and Technology University, resident

2004-2008	Tongji Medical College, Huazhong Science and Technology University, Master of Science
2005 – 2008	Union hospital Cancer Center, Tongji Medical College, Huazhong Science and Technology University, attending physician
2008 – present	Visiting scholar, Department of radiooncology, Saarland University Hospital, Homburg/Saar, Germany